Dynamic energy budget (DEB) parameter estimation for the globally invasive Quagga Mussel (*Dreissena rostriformis bugensis*)

T. Pu[a], S.S. Keretz[a], A.K. Elgin[b], C.M. Godwin[a], M.D. Rowe[c], H.J. Carrick[d], P.W. Glyshaw[c], R.M. Pietscher[b], and H.A. Vanderploeg[c]

[a] Cooperative Institute for Great Lakes Research, School for Environment and Sustainability, University of Michigan, Ann Arbor, MI, USA
[b] National Oceanic and Atmospheric Administration, Great Lakes Environmental Research Laboratory, Muskegon, MI, USA
[c] National Oceanic and Atmospheric Administration, Great Lakes Environmental Research Laboratory, Ann Arbor, MI, USA
[d] Department of Biology and Institute for Great Lakes Research, Central Michigan University, Mount Pleasant, MI, USA

Highlights

- Showed the need for a bioenergetic model specific to Quagga Mussel physiology.
- Analyzed dreissenid mussel physiology data collected within the last 20 years.
- Used selectivity coefficients to estimate environmentally available food density.
- Identified differences in parameters compared to other DEB database bivalves.
- Quagga Mussel parameter differences contribute to the species invasion success.

Abstract

Impacts of *Dreissena* spp. on infrastructure, nutrient cycling, and productivity in invaded ecosystems have been well-documented. These effects are influenced by mussel density, growth, and reproduction; therefore, there is a need to parameterize a dreissenid bioenergetic model that can be incorporated into lake management decision support tools. Since Quagga Mussels (*D. rostriformis bugensis*) are the most common dreissenid species in the Laurentian Great Lakes, we compiled existing data from the past 20 years of literature to estimate Dynamic Energy Budget (DEB) model parameters for Quagga Mussels to predict mussel growth, filtration, temperature dependence, and nutrient fluxes. Our estimations for shape coefficient, maximum reserve density, Arrhenius temperature, surface area-specific ingestion rate, and surface area-

specific searching rate were within the range of previously published DEB parameters for bivalves, with key differences that we relate to Quagga Mussel success in the Great Lakes through growth model simulations. Additionally, since dreissenids feed differentially on available prey, selectivity coefficients for common taxonomic algal groups and sizes were estimated which can be used to calculate effective food concentrations and estimate the environmentally available food density for Quagga Mussels. Finally, we developed an initial calibration of a DEB model in order to predict Quagga Mussel clearance rates in response to varying environmental conditions. Since field-collected data are not designed for precise parameter estimation, significant uncertainties in parameter estimates currently persist, highlighting the need for well-controlled laboratory experiments. The components of this model hold potential for integration into biogeochemical models to elucidate mussel effects on nutrient cycling and their response to future environmental changes. This integration enhances our understanding of ecosystem dynamics and can inform effective management strategies for invasive species in aquatic environments.

Keywords: bioenergetic modelling, selectivity coefficients, *Dreissena* physiology, DEB modelling

1. Introduction

Quagga and Zebra mussels (*Dreissena rostriformis bugensis and D. polymorpha*; herein dreissenids) have a well-documented history of negative impacts on their invaded environments. The impacts of a dreissenid invasion include increased water clarity (Fahnenstiel et al., 2010), altered plankton communities (Strayer et al., 1998), impacted food web structure (Madenjian et al., 2015), and increased toxic harmful algal blooms through selective filter feeding

(Vanderploeg et al., 2001). The biodiversity of invaded ecosystems, including native mollusks, macrophytes, and fish, is also affected by dreissenid introduction through both indirect and direct competition for food, resources, and habitat (Burlakova et al., 2000; Gobin et al., 2015; Hoyle et al., 2008). Human economics have been negatively affected by a dreissenid invasion due to increased costs in infrastructure maintenance and the increased frequency of toxic algae blooms in near-shore areas (Limburg et al., 2010; Prescott et al., 2014).

Zebra Mussels were introduced to the Laurentian Great Lakes in the mid-1980's and Quagga Mussels followed shortly after in the early 1990's (Hebert et al., 1989; Mills et al., 1993). Both species spread quickly to all five Great Lakes and the connecting waterways (Griffiths et al., 1991; Sturtevant et al., 2019). The dreissenid life cycle includes a planktonic veliger stage before the mussels settle in the benthos as juveniles and begin developing sexual maturity as small as 5 mm in length (Delmott and Edds, 2014; Juhel et al., 2003). While Quagga and Zebra Mussels have many similar characteristics, such as life cycle and prolific reproduction, the two species differ in habitat and physiological rates (Karatayev and Burlakova, 2022). For example, Quagga Mussels, compared to Zebra Mussels, are believed to grow faster and have higher filtration rates (Karatayev and Burlakova, 2022; Mills et al., 1993; Tang et al., 2014). Additionally, Quagga Mussels can grow and reproduce in colder temperatures, which has allowed them to expand their range to deeper habitats than Zebra Mussels (Karatayev et al., 2015; Karatayev et al., 2021). Therefore, any physiological modelling efforts for dreissenids in the Great Lakes should focus on Quagga Mussels, the now dominant dreissenid species throughout the region (Karatayev et al., 2022; Karatayev et al., 2020).

There is a need for a model that can predict dreissenid growth, feeding capacity, and reproduction within the Great Lakes aquatic ecosystem, which can then be incorporated into

biogeochemical models used for lake management decision support. Some dreissenid models covering these parameters exist (Bierman et al., 2005; Griebeler and Seitz, 2007; Karatayev et al., 2018; Madenjian, 1995; Rowe et al., 2017; Schneider, 1992); however, most focused on Zebra Mussels or used a simplified representation of Quagga Mussels. Potential methods for modelling organism growth and physiology include the International Biological Program and the scope for growth method, the metabolic theory of ecology, net-production models, species-specific models, and dynamic energy budget theory, DEB (van der Meer, 2006). The DEB theory developed by Kooijman (2010) led to a modelling framework that is widely applicable to a large variety of organisms and faunal groups (Lavaud et al., 2025). Briefly, four state variables are defined by the DEB theory: reserve, structure, reproduction buffer, and maturity. A calibrated model can be used in the prediction of any state variables under varying food levels and temperatures (Kooijman, 2010; Lika et al., 2011a). Therefore, DEB models can be used to model an organism's growth or can predict biomass changes in response to fluctuating environmental factors (Kooijman, 2010; Kooijman, 2020).

Over the past several years, DEB models have been used for a wide range of aquatic mollusk taxa, including the Grooved Carpet Shell (*Ruditapes decussatus*), Green-Lipped Mussel (*Perna canaliculus*), and Blue Mussel (*Mytilus edulis*) (Lanjouw et al., 2024; Ren et al., 2020; Saraiva et al., 2012). DEB models have also been used to investigate the ecology of aquatic invasive species to further our understanding of species' physiology that leads to invasion success (Augustine et al., 2014; Marn et al., 2022; Nepal et al., 2024). Some DEB model parameters have been estimated for Quagga Mussels (Huff, 2023); however, Huff (2023) primarily focused on a subset of Great Lakes mussels from Lakes Michigan and Huron. Despite the promise of DEB as a modelling framework, availability and applicability of empirical

measurements to inform the models is often limiting. A fully realized DEB model requires reliable estimates of the individual's life cycle, maintenance, and development as well as experimental data on growth rates, feeding rates (energy acquisition), and reproductive rates at various temperatures and food levels (Lika et al., 2011a; Marques et al., 2018). Most DEB parameters (*e.g.*, the fraction of reserve allocated to somatic maintenance (κ), volume-specific energetic cost for structure ($[E_G]$), and maturity levels (E_H^b and E_H^p)) are too abstract to measure directly through simple experiments. These parameters are typically estimated using the co-variation method (Lika et al., 2011a; 2011b). The co-variation method uses multiple physiological datasets simultaneously to minimize the distance between the data and model predictions and estimate complex parameters (Lika et al., 2011a). However, when available data are insufficient to achieve convergence with the co-variation method, a few parameters (*i.e.*, shape coefficient, surface-area specific maximum ingestion rate, Arrhenius temperature, etc.) can be approximated with data collected from well-designed experiments (Sarà et al., 2013). These parameters can then be used to make a calibrated model for specific physiological processes like an organism's clearance (filtration) and growth rates (Huff, 2023).

Numerous previous studies have summarized experimental results related to dreissenid mussel physiology (Bootsma and Liao, 2014; Karatayev and Burlakova, 2022; Karatayev et al., 2006; Karatayev et al., 2015; Ram et al., 2012). Past physiology studies have mainly focused on Zebra Mussels (Karatayev et al., 2006), although Quagga Mussels have become more prominent in recent literature (Elgin et al., 2022; Haltiner et al., 2023; Kemp and Aldridge, 2018; Vanderploeg et al., 2010). However, observational or experimental data that can be directly used for DEB parameter estimation are relatively scarce in dreissenid literature, as past dreissenid physiology experiments were not designed for the purpose of DEB model parameterization.

Therefore, the objectives of this study were to 1) analyze data collected from Quagga Mussel physiological experiments conducted between 2008 and 2023 by the NOAA Great Lakes Environmental Research Laboratory (GLERL) and published sources, 2) use existing physiological data specific to Quagga Mussels to estimate a few simple DEB parameters and 3) use the parameter estimates to predict Quagga Mussel clearance and growth rates. This study will highlight knowledge gaps in Quagga Mussel physiology literature, calculate the effective food concentration available to mussels in environments with variable algal compositions, provide DEB parameter estimates that can be used as a starting point for creating a fully calibrated Quagga Mussel DEB model, and provide a framework for estimating DEB parameters when a species has insufficient physiological data available to utilize the co-variation method.

2. Materials and methods

Existing experimental physiology data for Quagga Mussels were analyzed and then used to estimate the DEB model parameters shape coefficient, maximum reserve density, Arrhenius temperature, and maximum surface area-specific ingestion and searching rates. An explanation for how each dataset was used and a brief summary of each experiment's methods are provided below. Data sets are organized in chronological order.

2008 - 2011 NOAA GLERL Feeding Experiments - Maximum surface area-specific ingestion and searching rates were estimated using data from feeding experiments with Quagga Mussels (Vanderploeg et al., 2010) and Zebra Mussels (Vanderploeg et al., 2009). Quagga Mussels were collected from Lake Michigan (profunda type collected from 45 m depth; Vanderploeg et al., 2010). Zebra Mussel data were used to calculate comparative values for surface area-specific ingestion and searching rate. Zebra Mussels were collected from Saginaw Bay, Lake Huron (Vanderploeg et al., 2009). Feeding experiments for both Quagga and Zebra

mussels used similar methodology where 4-5 mussels were fed *Cryptomonas ozolini* (0.8 - 3.0 μg L^{-1} chlorophyll-*a* initial concentration) and allowed to filter feed for 2-3 hours. Experiments were conducted between May and November. Due to the differences in collection depth, experimental temperatures ranged between 2 and 7°C for Quagga Mussels and 5 and 25°C for Zebra Mussels (Vanderploeg et al., 2009; Vanderploeg et al., 2010). Both experiments normalized clearance rates to ash free dry weight (mg; AFDW). A note on terminology: we defined clearance rate (FI; L mg^{-1} hr^{-1}) as the volume of water being filtered and ingestion rate (IR; μg chl mg^{-1} hr^{-1}) as the amount of food being ingested. The chlorophyll measurement (μg chl) is assumed to represent food particle dry mass or food energy.

Respiration Experiments - Tyner et al. (2015) investigated Quagga Mussel respiration rates across temperatures ranging from 5 to 23°C. This data was used to calculate an Arrhenius temperature. Briefly, Tyner et al. (2015) conducted respiration experiments in both the lab (5 to 19°C) and with experimental chambers at 10 m depth in Lake Michigan (8 to 23°C). Mussels were collected from 10 m depth in Lake Michigan and acclimated at experimental temperatures for three hours prior to experimentation. Lab experiments were conducted for two hours in a closed chamber and initial and final dissolved oxygen concentrations were measured using a NeoFox Sport optical oxygen microsensor. The Lake Michigan experiments were conducted by placing a chamber with an attached Clark-type polarographic oxygen electrode (YSI model 600R Sonde) over a section of dreissenids attached to a rock's surface for 20-30 minutes. All respiration rates were normalized to mussel tissue dry weight (Tyner et al., 2015).

Length-Weight data - Elgin and Glyshaw (2021) published a dataset that provides Quagga Mussel shell length and tissue weight data collected between 2015 and 2023 from stations in Lakes Michigan, Huron, Ontario, and Erie. This dataset was used to calculate length-

weight regressions for mussels in high productivity (i.e., well-fed) and low productivity (i.e., starved) environments in order to estimate shape coefficient and maximum reserve density. To briefly summarize their methods: Quagga Mussels were collected from the lake bottom at each site and processed within 48 hrs of collection. Processing entailed measuring the maximum anterior-posterior length to the nearest 0.1 mm, separating all mussel tissue from the shell and drying the tissue at 60°C for at least 48 hrs and weighing to the nearest 0.1 mg, and drying the shell at room temperature for at least 24 hrs and weighing to the nearest 0.1 mg.

Elemental Composition - Carter et al. (2023) and Vanderploeg et al. (2017) measured C, N, and P content in Quagga and Zebra mussel tissue, respectively. In both studies, mussel tissue was first dried at 60°C and subsamples were used to estimate particulate organic carbon (POC), particulate organic nitrogen (PON), and P. For POC and PON, tissue subsamples were analyzed using an Elantech EA1100 CHN Analyzer (Vanderploeg et al., 2017). For P, the tissue subsamples were combusted and analyzed spectrophotometrically on a Seal Quaatro continuous segmented flow analyzer (Carter et al., 2023). Zebra Mussels were collected from Gull Lake, Michigan (Horst et al., 2014; Vanderploeg et al., 2017) and Quagga Mussels were collected from western Lake Erie (Carter et al., 2023).

2018 Feeding Experiments - Vanderploeg et al. (2023) and Carrick et al. (2023) conducted feeding experiments with Quagga Mussels between May and October in 2018. These experimental results were used to estimate selectivity coefficients (organism preference for certain foods) and were also used as a comparison to our model predictions of Quagga Mussel clearance and ingestion rates. Briefly, mussels were collected from western Lake Erie and experiments were conducted in 20 L buckets containing 10 L of lake water with naturally occurring seston. Algal classes within the lake seston were measured before and during the

experiment at one-hour intervals over a 2–4-hour period. Incubation and experimental temperatures were kept consistent with values recorded during mussel collection and ranged from 8 to 25℃. At the conclusion of each experiment, mussels were removed, each bucket was mixed, and final samples were taken. The following variables were measured: total and size-fractionated chlorophyll in pico-, nano-, and microplankton size ranges (0.2-2 μm, 2-20 μm, 20-200 μm size ranges, respectively) and total and type-fractionated algal type (green algae, blue-green algae, diatoms, and cryptophytes). Algal classes were determined by spectral fluorometry (FluoroProbe data; Vanderploeg et al., 2023) and microscopy (Carrick et al., 2023). Algal size was also determined by microscopy (Carrick et al., 2023).

Chlorophyll and POC data in the Great Lakes – Chlorophyll-*a* and particulate organic carbon (POC) concentration data were collected in Lake Huron's Saginaw Bay, Lake Erie, and Lake Michigan as part of a long-term lower food web research project conducted by GLERL (NOAA GLERL, 2024). These data were used as a proxy measurement for food energy content available to mussels from natural seston in Lakes Huron and Michigan. Methods for data collection in Lake Erie are presented in Boegehold et al. (2023) and methods for data collection in Lake Michigan are presented in Pothoven and Vanderploeg (2020). Briefly, water column samples were collected using a 5 L vertical Niskin bottle. To analyze POC, water samples were collected onto glass fiber filters, acidified with 10% HCl, and dried at 70℃ for 24 hr before being quantified on a PerkinElmer 2400 or a Carlo-Erba 1110 CHN elemental analyzer (Boegehold et al., 2023; Hedges and Stern, 1984; Pothoven and Vanderploeg, 2020). Chlorophyll-*a* concentrations were determined by filtering a known volume of lake water onto 47 mm Whatman GF/F glass fiber filters (Cytiva Life Sciences). Chlorophyll-*a* was extracted from samples using dimethylformamide and then cooled to room temperature and mixed by

vortex before being quantified using a 10AU fluorometer (Turner Designs) (Boegehold et al., 2023; Pothoven and Vanderploeg, 2020; Speziale et al. 1984).

2.1 Dreissenid physiology

2.1.1 Length-weight regressions

Two methods were used to calculate length-weight regressions for Quagga Mussels assumed to be either well-fed or starved from the Quagga Mussel length and weight data published by Elgin and Glyshaw (2021). For the first method, we used all length and weight measurements available from Lakes Ontario, Erie, Huron, and Michigan collected between 2015 and 2023 (Elgin and Glyshaw, 2021). The top 5% quantile, regardless of site or lake, was assumed to represent well-fed mussels while the lowest 5% quantile was assumed to represent mussels that were either starving or were close to starving. For both groups, we applied a standard major axis regression with intercept = 0.

The second method was used to check the relevance of the quantile values against known high and low productivity sites. Therefore, length and weight data came from sites where mussels were expected to be well-fed (high productivity sites) or near starving (low productivity sites). Mussel length and dry tissue weight data collected in 2019 from shallow sites, with observed levels of high productivity, in Lake Erie (depth <30 m, n = 6 sites) represented the well-fed mussel group. Mussel length and dry tissue weight collected in 2021 from mid-depth sites with low levels of productivity, in Lake Michigan (depth 30-90 m, n = 8 sites), represented the starving mussel group. For the starving and well-fed groups, we applied a standard major axis regression with intercept = 0.

For both methods, we assumed that weight has a linear relationship with the cube of mussel shell length. Following the isomorphy assumption discussed in the standard DEB theory

(Kooijman, 2010), the structural volume is the cube of structural length, which is some proportion of physical length (*e.g.*, maximum anterior-posterior length). Additionally, we assumed that the structural length can be converted to structural dry weight with a fixed density. We made these assumptions because analyzing the relationship between dry weight and shell length cubed is more informative for estimating DEB-specific parameters.

2.1.2 Weight conversions

The dataset published by Elgin and Glyshaw (2021) was also used to calculate a conversion factor from tissue dry weight, shell weight, and tissue wet weight (whole mussel wet weight - shell weight) to tissue ash free dry weight (AFDW). Major axis linear regression was the chosen regression method, because it considers uncertainties in both the independent and dependent variables; and therefore, the conversion factor is not limited to predicting from one axis to another.

2.1.3 Selectivity coefficient (w_i') and effective food concentration (EFC)

Selectivity coefficients, as detailed by Vanderploeg et al. (1984) for copepods, estimate organism preference for certain food types based on their clearance rate. To calculate selectivity coefficients for Quagga Mussels, we analyzed clearance rate data from a series of feeding experiments conducted in 2018 (Carrick et al., 2023; Vanderploeg et al., 2023). These experiments measured Quagga Mussel clearance rates on naturally occurring size classes of hetero- and photo-trophic plankton (pico 0.2-2 μm, nano 2-20 μm, and micro 20-200 μm, respectively), and taxonomic groups including both heterotrophic (prasinomonads, ciliates, chrysomonads, and dinoflagellates) and phototrophic (diatoms, chlorophytes, cryptophytes, and cyanobacteria) groups of plankton present in the lake. Selectivity coefficients (w_i') for different food sizes and types were then calculated using the following equation:

1. $w_i' = FI_i \,/\, FI_{pref}$

Where w_i' is the selectivity coefficient of interest given food fraction 'i'. FI_i is the clearance rate for a particular food type/size and the FI_{pref} is the clearance rate for the most preferred food type/size. Subsequently, an effective food concentration (EFC; µg chl L^{-1}) based either on food type or size was calculated by taking the sum of the concentration of each food type/size (X_i) multiplied by its associated selectivity coefficient (w_i').

2. $EFC = \sum (w_i' X_i)$

2.1.4 Elemental composition

We estimated the elemental composition of Quagga (Carter et al., 2023) and Zebra mussel (Vanderploeg et al., 2017) tissue. Elemental composition was calculated as chemical indices per C mol of dry tissue and as a weight per organism dry tissue weight. For reference, a standard DEB model assumption about the elemental composition of microorganisms (Kooijman, 2010) and the Redfield ratio, the elemental composition of marine phytoplankton (Anderson, 1995; Redfield, 1933), are also presented. Anderson (1995) updated the Redfield ratio with H and O and came up with the marine phytoplankton molecular formula $C_{106}H_{175}O_{42}N_{16}P$. All datasets were compared by converting the data into element weight versus total dry tissue weight. For the Redfield ratio, we derived the dry tissue mass by assuming the object is composed of only C, H, N, O, and P.

2.2 DEB parameter estimation

DEB parameters are commonly determined using the covariation method, a method established by Lika et al. (2011a; 2011b) that minimizes the loss function or the distance between the data and model predictions using multiple physiological datasets simultaneously to estimate parameters for a species of interest. For cases when the available data are insufficient to

constrain the covariation method, there are still some DEB parameters that can be calculated using data from controlled experiments (Sarà et al., 2013; van der Veer et al., 2006). Although the analyzed experiments were not specifically designed to inform DEB parameters, they still provide useful information on possible parameter ranges. This manuscript follows the DEB terminology and symbology previously established in van der Veer et al. (2006). Brief descriptions to give biological context for each of the DEB parameters estimated are provided in the corresponding sections below.

2.2.1 Shape coefficient (δ_M)

Shape coefficient (δ_M) is the ratio between the abstract DEB structural length (L) and the physical length (L_{phy}) of the organism (usually shell length for mussels).

3. $\delta_M = L \,/\, L_{Phy}$

Structural length cannot be measured directly but it is related to the organism's dry weight (W_d) (Kooijman, 2010) by the following equation:

4. $W_d = d_V \, L^3 (1 + f\omega)$

Where d_V represents the density of dry structure (0.09 g cm^{-3} for bivalves; Kooijman, 2023; Ricciardi and Bourget, 1998), f represents the scaled functional response describing the abundance of food (a unitless variable that commonly ranges between 0 (starving) and 1 (well-fed)), and ω represents the contribution of reserve to weight. The equation is then rearranged to include physical length (L_{phy}) and shape coefficient (δ_M):

5. $W_d = d_V \, (\delta_M L_{phy})^3 \, (1 + f\omega)$

If a regression using dry tissue weight (or better, ash free dry weight to exclude salt contribution) as the dependent variable and shell length cubed as the independent variable, the slope of the regression is equal to $d_V \, {\delta_M}^3 (1 + f\omega)$. The slope is then used to solve for δ_M. Specifically, we

used the shell length and dry weight regression slope calculated from starving Quagga Mussels in section 2.1.1:

6. $\delta_M = (slope\ /\ (1 + f\omega)\ d_V)^{1/3}$

By using length-weight data from a starving mussel population, we assumed the functional food response term ($f\omega$) was equal to 0.

2.2.2 Maximum reserve density ($[E_M]$) and maximum surface area-specific assimilation rate ($\{\dot{p}_{Am}\}$)

The maximum reserve density ($[E_m]$; J cm^{-3}) is the maximum amount of reserve E (Joules) for a specific structure volume V (cm^3) and occurs when an organism is well fed (Kooijman, 2010). Maximum reserve density is a constant value regardless of the organism's age and is the ratio between the maximum reserve energy and the structural volume of the organism. To estimate the maximum reserve density, the difference in energy content between a well-fed individual and a starved individual of the same size is calculated:

7. $[E_m] = \left(\frac{W_d}{L^3}|_{high\ food} - \frac{W_d}{L^3}|_{low\ food}\right) * 23\ J\ mg^{-1}$

Where energy content for well-fed (high food) and starved (low food) individuals was estimated using the Quagga Mussel length-weight regressions calculated in section 2.1.1. The 23 J mg^{-1} (Table 1) is the typical DEB energy density for reserve and is calculated by:

8. $\frac{\mu_E}{w_E} = \frac{550000\ J\ mol^{-1}}{23.9\ g\ mol^{-1}}$

Where μ_E is the typical energy content for reserve and is estimated based on the typical macromolecular chemical composition per C-mol of reserve and the energy potential (Kooijman, 2010). The variable w_E is the molecular weight (per C-mol of) for reserve, assuming the reserve is described by an elemental composition of C: H: O: N = 1: 1.8: 0.5: 0.15 (Table 1).

Using the $[E_m]$ estimation, other parameters such as surface-area-specific maximum assimilation rate ($\{\dot{p}_{Am}\}$; J d^{-1} cm^{-2}) and volume-specific somatic maintenance rate ($[\dot{p_M}]$; J d^{-1} cm^{-3}) can also be estimated with the following:

9. $\{\dot{p}_{Am}\} = [E_m] * \dot{v}$

Where $\dot{v}$ is energy conductance and is assumed to be equal to 0.02 cm d^{-1} for most DEB organisms.

10. $[\dot{p_M}] = \frac{\kappa\{\dot{p}_{Am}\}}{z}$

Where κ is the fraction of mobilised reserve allocated to soma, a unitless parameter, and is estimated to be 0.993 for Zebra mussels in AmP collection (AmP Collection, 2024). We assumed the same value for Quagga Mussels. The parameter z is the zoom factor (cm) and is estimated 0.879 for Zebra mussels in the AmP collection database (AmP Collection, 2024). We assumed that Quagga Mussels have a comparable zoom factor to Zebra mussels because of their similar ultimate size. We scaled the zoom factor for Quagga Mussels by accounting for the differences in shape coefficients:

11. $Z_{QM} = Z_{ZM} \frac{\delta_{MQM}}{\delta_{MZM}}$

The relationship between $\{\dot{p_{Xm}}\}$ and $\{\dot{p_{Am}}\}$ is often represented by the digestion efficiency of food to reserve (κ_X):

12. $\kappa_X = \frac{\{\dot{p_{Am}}\}}{\{\dot{p_{Xm}}\}}$

2.2.3 Arrhenius temperature (T_A)

Arrhenius temperature (T_A ; K) is the species-specific effect of temperature on physiological rates, typically derived from plotting any metabolic rate against the inverse of

absolute temperature (Lika et al., 2011a; van der Veer et al., 2006). The temperature response of a metabolic rate can be described by the following equation:

13. $ln\left(\dot{k}(T)\right) = ln\,(\,\dot{k}_{ref}) + T_A * (\frac{1}{T_{Ref}} - \frac{1}{T})$

Where $\dot{k}(T)$ is the metabolic rate at temperature T and $\dot{k}_{ref}$ is the metabolic rate at reference temperature T_{Ref} in Kelvin. In DEB, T_{Ref} is 20°C (293.15 Kelvin). T_A is Arrhenius temperature, which is a constant that describes the temperature response of metabolic rate. The DEB theory assumes that the temperature response of all the metabolic processes in one organism are the same. The data we analyzed are within temperature tolerance range, so they should change monotonically according to this relationship. If $ln(\dot{k}(T))$ is plotted against $(\frac{1}{T_{Ref}} - \frac{1}{T})$, the slope is equal to T_A and the intercept is $ln\,(\,\dot{k}_{ref})$. In other words, T_A and reference metabolic rate can both be obtained from such a regression. We calculated T_A using Quagga Mussel respiration rates from Tyner et al. (2015) and Quagga Mussel clearance rates from Vanderploeg et al. (2010).

Once T_A is estimated, metabolic processes can be temperature corrected according to Eq. 13. For simpler representation, we define the temperature correction function as:

14. $tempcorr(T) = T_A * (\frac{1}{T_{Ref}} - \frac{1}{T})$

The result of which is a temperature correction factor that will be 1 at the reference temperature (20°C). It will be less than 1 if the temperature of interest is less favored than 20°C (usually under colder conditions) and it will be greater than 1 if the temperature is more favored than 20°C.

2.2.4 Surface-area specific maximum ingestion rate ($\{\dot{p}_{Xm}\}$) and maximum surface-area specific searching rate ($\{\dot{F}_m\}$)

In DEB theory, ingestion rate (IR) is the amount of food (or energy) being ingested per time and is described by a saturation curve:

15. $IR = \dot{p}_X = \{\dot{p}_{Xm}\} L^2 f$

Where $\{\dot{p}_{Xm}\}$ (J d^{-1} cm^{-2}) represents the maximum surface-area specific ingestion rate which describes the maximum amount of food a mussel can ingest and is measured by culturing mussels in a constant and abundant food environment. The variable L (cm) represents organism structural length and f is the unitless functional response term:

16. $f = \frac{X}{X+K}$

Where X (J L^{-1}) represents the food concentration in the environment and K (J L^{-1}) represents the half-saturation coefficient. The half-saturation coefficient (K) represents the food concentration at which half of the maximum ingestion rate is reached. It is related to the maximum surface-area specific searching rate ($\{\dot{F}_m\}$; L d^{-1} cm^{-2}) and $\{\dot{p}_{Xm}\}$ (Kooijman, 2010). The parameter $\{\dot{F}_m\}$ describes the maximum amount of water filtered (cleared) per structural area, which typically occurs at a very low food level.

17. $K = \{\dot{p}_{Xm}\} / \{\dot{F}_m\}$

These parameters can be estimated from a mussel feeding experiment performed at different food concentrations (visualized for reference in Figure 1). Specifically, we estimated $\{\dot{p}_{Xm}\}$ and $\{\dot{F}_m\}$ for both Quagga and Zebra mussels from previous experiments where mussels were fed *Cryptomonas ozolini* at different concentrations (Vanderploeg et al., 2009; Vanderploeg et al., 2010).

2.3 Model predictions

2.3.1 Converting food measurements to joules

Chlorophyll concentration was used as a proxy measurement for algae abundance in both the 2008 and 2018 feeding experiments (Carrick et al., 2023; Vanderploeg et al., 2023; Vanderploeg et al., 2009). This provides insight regarding the amount of food available for dreissenids; however, the DEB model specifically needs information about food energy. Therefore, chlorophyll concentrations were converted to an available energy content in J.

Chlorophyll (chl) and POC data were collected by GLERL in Lake Huron's Saginaw Bay, Lake Erie, and Lake Michigan as part of a long-term lower food web research project (NOAA GLERL, 2024). Data from all three locations were used together. First, we converted chlorophyll to POC:

18. $\log_{10}(POC) = 0.76 * \log_{10}(chl) - 0.82$

Where POC is measured in mg C L^{-1} and chlorophyll concentration is measured in µg chl-*a* L^{-1}. The details of this regression are included in supplementary information (See Supplementary Material Figure 1).

We assumed food particles are measured as particulate organic matter (so that POC represents the carbon content in the food particles) and that they have a constant energy density as described in Table 1. Thus, we calculated the food energy from the previously calculated POC. Furthermore, when an experiment uses a mixture of different food types, it is important to distinguish them. For example, cyanobacteria can provide as much chlorophyll as cryptophytes but, it is less favored by dreissenid mussels. One way to compensate for this problem is to use the effective food concentration method described in section 2.1.3.

2.3.2 Modelling Vanderploeg et al. (2023) feeding experiments

The DEB parameters estimated in section 2.2 were used to make predictions about Quagga Mussel clearance and ingestion rates. Model predictions were then compared to data

collected during the 2018 feeding experiments (Carrick et al., 2023; Vanderploeg et al., 2023). Once the food concentration was converted to a single variable (J L^{-1}), the ingestion rate was modeled using Eqs. 15 and 16. To calculate the amount of water being cleared (FI; mL hr^{-1} mg^{-1}), the modeled ingestion rate was divided by the effective food concentration:

19. $FI = IR / X$

Parameter sensitivity of the modeled ingestion rate was further explored by using several plausible combinations of $\{\dot{F}_m\}$ and $\{\dot{p}_{Xm}\}$. These plausible combinations come from $\{\dot{F}_m\}$ and $\{\dot{p}_{Xm}\}$ estimations previously made for other mollusk species (Table 5) and can be summarized as "low" and "high" predicted ingestion levels (Table 2).

2.3.3 Parameter impacts on mussel growth rate predictions

The DEB parameters estimated in section 2.2 were also used to compare Quagga and Zebra mussel growth based on their different parameter estimates. Specifically, we used estimates of DEB parameters for Quagga and Zebra mussels to compare parameter effect on organism growth. We highlighted the differences between 1) their temperature response by simulating growth with different estimations of Arrhenius temperature (T_A) and 2) food uptake rates by manipulating estimates of maximum surface-specific clearance rate ($\{\dot{F}_m\}$). We were unable to estimate all the necessary parameters due to missing corresponding experimental results, such as κ (allocation fraction to soma) and E_G (volume-specific cost for structure, including overhead costs). Therefore, for the missing parameters, we used estimates that were calculated for Zebra Mussels from the AmP Collection (2024), assuming that these values would be similar between Zebra and Quagga mussels (See Supplementary Material Table 1).

To simulate mussel growth, we started the growth curves with a 1 cm shell-length mussel, a length at which the mussel should already be mature (Delmott and Edds, 2014) and

therefore maturation is equal to the maturity at puberty. The initial reserve is a fraction of maximum reserve at that structural length and the fraction is determined by the functional response f (Eq. 16) for each simulation. The specification of constant temperature and food level for a mature mussel allows for a growth curve simulation using the von-Bertalanffy growth scenario described in Kooijman (2010).

To simulate a more realistic environmental condition for all simulations, the average temperature and chlorophyll concentrations were obtained from Lake Ontario in 2018-2019 (Elgin et al., 2022). The average temperature in Lake Ontario from June 2018 to May 2019 was 3.76°C at 90 m depth, which we assumed as our environmental temperature for all simulations. Additionally, at 90 m depth the average chlorophyll concentration in Lake Ontario from June 2018 to May 2019 was 0.50 µg L^{-1}. Using the conversion process explained in section 2.3.1, the chlorophyll concentration value was converted to 3.9 J L^{-1} which corresponds to an f of 0.37.

3. Results and Discussion

3.1 Quagga Mussel physiology

3.1.1 Length-weight regressions

Two methods were used to calculate a Quagga Mussel length-weight relationship, both of which yielded similar slope values (Figure 2). The first method assigned well-fed and starving groups based on the highest 5% and lowest 5% quantiles. The resulting slopes were 3.18 * 10^{-3} ± 1.20 * 10^{-5} g cm^{-3} (n = 3039, df = 1) for the top 5% (well-fed individuals) and 1.03 * 10^{-3} ± 1.06 * 10^{-5} g cm^{-3} (n = 3039, df = 1) for the lowest 5% (starved individuals) (Figure 2b). These slopes (and their uncertainties) were used to calculate DEB parameters shape coefficient (δ_M; section 3.2.1) and maximum reserve density ($[E_m]$; section 3.2.2). The second method assigned well-fed and starving designations based on site location and observed site productivity. With the site

method, the slopes were $3.31 * 10^{-3} \pm 8.56 * 10^{-5}$ g cm^{-3} (n = 150, df = 1) for mussels at high productivity sites (Lake Erie 2019, well-fed) and $1.30 * 10^{-3} \pm 2.03 * 10^{-5}$ g cm^{-3} (n = 199, df = 1) for mussels at low productivity sites (Lake Michigan 2021, starved; Figure 2a).

The two methods for determining well-fed versus starved individuals produced similar results, although the quantile method resulted in slightly smaller slopes than the site method. The quantile method used the full length-weight dataset from Lakes Huron, Ontario, Michigan, and Erie in order to capture the wide range of variability expressed among Quagga Mussels in the Great Lakes. While Lake Michigan 2021 was specifically selected to represent a low-productivity environment, oligotrophic conditions have been reported offshore in Lakes Huron (excluding Saginaw Bay; Stadig et al., 2020) and Ontario (Holeck et al., 2019) as well, accounting for similar length and weight measurements across all lakes. It should also be noted that, while using the quantile method, the lowest 5% quantile had a tighter distribution than the highest 5% quantile, which suggests that the weight of a starved mussel consists mainly of structure and has a tighter relationship with mussel shape. Alternatively, the well-fed mussel (represented by the highest 5% quartile) consists of both structure and reserve. Since reserve density fluctuates with environmental conditions, it is possible that the well-fed group is not truly well fed, because the environmental conditions can fluctuate throughout the year, leading to either loss of reserve mass or larger individual variation (in reserve mass) (Kooijman, 2010; Lika and Kooijman, 2011).

3.1.2 Weight conversion

Weight conversions are necessary when certain weight metrics are not available within a dataset. For example, AFDW is commonly used by DEB because it gives an accurate representation of tissue composition (Kooijman, 2010). However, measuring shell weight, dry

weight and AFDW, requires sacrificing mussels which may not be ideal for a long-term growth experimental design. Here, we provide conversion factors summarized from Quagga Mussel tissue measurements collected throughout the Great Lakes between 2015 and 2023 (Elgin and Glyshaw, 2021; Figure 3 and Table 3). Table 3 provides the conversion equations for each weight metric we measured, converting tissue dry weights, tissue wet weights, and shell weights to and from AFDW. Although the relationships between tissue ash free dry weight and tissue wet weight, AFDW and shell weight are more scattered, they still provide useful information and allow weight conversions in numerical models when direct measurement is not available.

3.1.3 Selectivity coefficients

Using microscopy data collected by Carrick et al. (2023), mean Quagga Mussel clearance rates were 9.36 ± 2.13 mL mg^{-1} hr^{-1} for heterotrophic microplankton (20-200 μm) and 15.66 ± 1.63 mL mg^{-1} hr^{-1} for heterotrophic nanoplankton (2-20 μm; Figure 4a). For the phototrophic plankton size classes, the mean Quagga Mussel clearance rates were 10.66 ± 2.00 mL mg^{-1} hr^{-1} for the microplankton, 18.47 ± 2.36 mL mg^{-1} hr^{-1} for the nanoplankton, and 6.03 ± 1.07 mL mg^{-1} hr^{-1} for the picoplankton (0.2-2 μm; Figure 4a). The selectivity coefficient (w_i') was set to 1 for the phototrophic nanoplankton size class (Table 4), as it had the highest observed mean clearance rate.

When calculated for different algal types, clearance rates were calculated using both FluoroProbe data and microscopy data collected by Vanderploeg et al. (2023) and Carrick et al. (2023), respectively. The results for several categories of phototrophic plankton (i.e., diatoms, chlorophytes, cyanobacteria) were confirmed using both fluorometric (Fluoroprobe) and microscopic analysis of experimental samples (Vanderploeg et al. 2023). Mean clearance rates were low for cyanobacteria when calculated with FluoroProbe data (0.42 ± 1.18 mL mg^{-1} hr^{-1}) or

509 microscopy data (-0.89 ± 3.01 mL mg^{-1} hr^{-1}; Figure 4b). Using microscopy data, clearance rates
510 were highest for taxonomic groups prasinomonids (21.15 ± 3.34 mL mg^{-1} hr^{-1}) and cryptophytes
511 (23.88 ± 3.45 mL mg^{-1} hr^{-1}; Figure 4b). That said, interpretation of fluorometric data was
512 complicated by the fact that most algal groups support suites of pigments that are not easily
513 characterized by the finite number of pigments recognized and bundled by the Fluoroprobe
514 meter. For instance, the brown algal group includes cryptophytes and dinoflagellates, so there is
515 not a simple method for disentangling these groups without microscopic analysis (see Garrido et
516 al. 2019). The selectivity coefficient was set to 1 for cryptophytes as this taxonomic group had
517 the highest observed mean clearance rate (Table 4).
518 The selectivity coefficient can be used to calculate EFC (effective food concentration), a
519 single estimate of food availability from a mixture of different food types, for the specific
520 purposes of DEB modelling. Quagga Mussels in Lake Erie, from the set of experiments
521 performed (Carrick et al., 2023; Vanderploeg et al., 2023), selectively filtered for nano-sized (2-
522 20 μm) heterotrophic protists (prasinomonads) and phototrophic algae (cryptophytes), while
523 selectively avoiding cyanobacteria (primarily *Microcystis* with lesser densities of *Anabaenopsis*
524 and *Planktothrix*) (Figure 4a, 4b). Carrick et al. (2023) reported and Figure 4 confirmed the
525 following order of preference for common algal taxonomic groups: cryptophytes > diatoms >
526 chlorophytes > cyanobacteria. These general preferences are also reported in multiple previous
527 studies (Tang et al., 2014; Vanderploeg et al., 2001; Vanderploeg et al., 2017; Vanderploeg et
528 al., 2014) and give further guidance for calculating EFC. For example, cyanobacteria, which
529 often occurs as toxic genera such as *Microcystis*, has a low selectivity coefficient and a small
530 contribution to the EFC. Alternatively, cryptophytes, diatoms, and small chlorophytes are
531 preferred food types for dreissenid mussels (Carrick et al., 2023; Tang et al., 2014; Vanderploeg

et al., 2009; Vanderploeg et al., 2001; Vanderploeg et al., 2017; Vanderploeg et al., 2014) resulting in high selectivity coefficients and large contributions to the EFC.

The size structure analyzed in the present study consisted of pico-, nano-, and microplankton size categories. Important size categories for food have been >53 µm, a size category that *Microcystis* colonies are typically found in Saginaw Bay and Lake Erie (Vanderploeg et al. 2001, 2009) and 80 µm, the upper size limit of *Microcystis* colonies that Zebra Mussels can ingest (White and Sarnelle, 2014). Numerical estimates for organism preference of certain food types and sizes allow us to make assumptions about dreissenid ingestion when given natural seston or a wide variety of different food types. Knowing the algal (and heterotrophic plankton) and size structure is particularly important for predicting the impacts of dreissenids.

3.1.4 Elemental composition

There are some differences between the commonly acknowledged values for living microorganisms and the Quagga and Zebra mussel tissues collected in the field (Table 1). For instance, the N content for Quagga and Zebra mussel tissues are higher than the Redfield ratio, while the P content is lower (Table 1; Anderson, 1995; Redfield, 1958). With robustly measured elemental composition (C, H, N, O, and P) of mussel tissues, or more specifically, tissue separated as somatic, reserve, and feces tissue, the standard DEB model could be further adapted to simulate the impact dreissenid mussels have on ecosystem biogeochemistry.

3.2 DEB parameter estimation

3.2.1 Shape coefficient (δ_M)

Using the lowest 5% quantile to represent starving Quagga Mussels, we estimated δ_M = 0.225 ± 0.05 g cm^{-3}. For Lake Huron and Lake Michigan Quagga Mussels, Huff (2023)

estimated δ_M to be 0.34, which is slightly larger than the value calculated in the current study. Compared to the current study, which used starving mussel AFDW collected from all five Great Lakes to estimate δ_M, Huff (2023) estimated δ_M using mussel wet weights from only Lakes Michigan and Huron and did not differentiate between starved and fed individuals, likely leading to the increased estimate. For additional comparisons, shape coefficients for other bivalve species range from 0.25 to 0.642 (Table 5; AmP Collection, 2024; Lanjouw et al., 2024; Ren et al., 2020; Saraiva et al., 2011). Shape coefficient naturally varies among mussel species based on their overall shape and how physical length is measured. However, the method for calculating shape coefficient also makes a difference. While shape coefficient is determined using length and body mass data, it is preferred, if possible, to account for an organism's structural mass only, excluding the mass contributed by reserves and reproductive systems (van der Veer et al., 2006). However, this is challenging to achieve since somatic mass and gonadal mass do not directly correspond to structural and reproductive components. Measuring body mass after spawning ensures the body mass is focused on organism structure. We assumed that using length and weight data from starving mussels would approximate a measurement of organism structure. Similarly, for all organisms, shape coefficient is largely dependent on when (in the organism's life cycle) the mass and length measurements were collected (van der Veer et al., 2006).

3.2.2 Maximum reserve density ($[E_M]$) and maximum surface area-specific assimilation rate ($\{\dot{p}_{Am}\}$)

We estimated $[E_m]$ = 4,516.7 ± 33.6 J cm^{-3} from the length-weight regressions of well-fed and starving Quagga Mussels (see section 3.1.1 and Table 5). Long-term growth experiments that either starve or over-feed Quagga Mussels are rare, particularly those conducted in sufficiently controlled environments (constant food and constant temperature). One notable

attempt was conducted by Zalusky (2021), who maintained experimental conditions for 231 days at 4°C. However, to date, no Quagga Mussel starvation and overfeeding growth experiments have been conducted with the purpose of capturing the maximum reserve density. As a proxy, $[E_m]$ can be approximated using field data by analyzing the difference between well-fed and starved mussels (Huff, 2023). Few studies have reported estimates for $[E_m]$, but Huff (2023) estimated $[E_m]$ at 3,520 J cm^{-3} for Quagga Mussels collected from Lake Michigan and Lake Huron, where mussels with high tissue condition (high weight per unit length) were considered well-fed and mussels with low tissue condition were considered starved. In our study, we used data from a broader population of Great Lakes mussels that included very high mass density individuals collected from Lake Erie in 2019 (Elgin and Glyshaw, 2021), which could explain our slightly higher estimation for $[E_m]$. Our estimate can be higher, but is overall similar in magnitude to values reported for various marine bivalves (2,080 to 4,835 J cm^{-3}; Ren et al., 2020; van der Veer et al., 2006; See Supplementary Material Figure 2). Our estimate is also higher than $[E_m]$ estimates for mollusk species native to the Great Lakes (*Elliptio complanata*, *Obliquaria reflexa*, and *Truncilla truncata*; Table 5). A lower estimate for $[E_m]$ indicates an increased stress response when environmental food concentration is low.

Since mussel condition varies over the course of the season (Glyshaw et al., 2015), it is important to sample mussels at their peak body mass. The Lake Erie 2019 mussels were sampled in July, which is during peak reproduction and body condition (Elgin et al., 2023). However, using field-collected mussels to estimate reserve density under starved and well-fed conditions can lead to over- or under-estimates of this parameter. While food levels can be very low in offshore, oligotrophic systems, the mussels are not experiencing true starvation conditions, which will result in an overestimate of the mass density and an underestimate of reserve density.

Although Lake Erie mussel have high mass density among Great Lakes mussels, it is still possible that these mussels could have experienced some level of food limitation due to presence of cyanobacteria (Vanderploeg et al., 2023) or episodes of high turbidity (Elgin et al., 2023) and that they were not reaching their full reserve potential, leading to further uncertainties when estimating $[E_m]$. Another potential cause for error comes from estimating the energy density from dry weight density, where values from the reserve column in Table 1 are used. This assumes the C-mol content of the reserve mass and assumes an energy density of 550,000 J C-mol^{-1}. Although Kooijman (2010) suggests these are good estimations for general organisms, caveats for field-collected Quagga Mussels have not yet been considered.

Based on the $[E_m]$ estimation, we also calculated $\{\dot{p}_{Am}\}$ to be 90.33 J d^{-1} cm^{-2} and $[\dot{p}_M]$ to be 154.21 J d^{-1} cm^{-3} (Table 5). Our estimate for $\{\dot{p}_{Am}\}$ is very similar to other estimates for mollusk species (see Supplementary Material Figure 2). For example, Huff (2023) estimated a $\{\dot{p}_{Am}\}$ of 78.2 J d^{-1} cm^{-2} for Lake Huron and Michigan Quagga Mussels and the AmP collection (2024) reported a $\{\dot{p}_{Am}\}$ estimate of 85.0 J d^{-1} cm^{-2} for Zebra Mussels. For other marine mollusk species, $\{\dot{p}_{Am}\}$ ranged from 3.2 to 109.2 J d^{-1} cm^{-2} (Table 5; AmP Collection, 2024; Ren et al., 2020). Mollusk species native to the Great Lakes (*Elliptio complanata*, *Obliquaria reflexa*, and *Truncilla truncata*) have lower $\{\dot{p}_{Am}\}$ per area than either Quagga or Zebra mussels, meaning the native species do not filter and assimilate food as efficiently as the invasive mussels (Table 5; AmP Collection, 2024).

3.2.3 Arrhenius temperature (T_A)

Tyner et al. (2015) conducted experiments on Quagga Mussel respiration rates at temperatures ranging from 5 to 23°C. Based on the regression equation from these respiration

data (Figure 5), the temperature response of oxygen consumption rate (or oxygen flux in DEB, JO) is summarized with the following:

$$20.\ ln\left(JO(T)\right) = (-3.10 \pm 0.09) + (5969.92 \pm 801.99) * (\frac{1}{T_{Ref}} - \frac{1}{T})$$

The T_A is the slope, 5,969.92 ± 801.99 K and the oxygen consumption rate at reference temperature 20°C is the exponential of the intercept 0.0452 ± 0.0452 μmol hr^{-1} mg dry $weight^{-1}$.

Alternatively, based on the regression equation using clearance data from Vanderploeg et al. (2010) (Figure 6), the temperature response of Quagga Mussel clearance rate (FI) is summarized by:

$$21.\ ln\left(FI(T)\right) = (3.13 \pm 0.17) + (2551.98 \pm 1266.07) * (\frac{1}{T_{Ref}} - \frac{1}{T})$$

The T_A for Quagga Mussel water clearance is the slope, 2,552 ± 1266 K, and the water clearance rate at reference temperature 20°C is the exponential of the intercept, 22.96 ± 3.82 mL hr^{-1} mg dry $weight^{-1}$.

The T_A estimated using the Tyner et al. (2015) respiration data is a similar estimate to other mollusk species like Asian Clams (*C. fluminea*), Blue Mussels, Soft-shell Clams (*M. arenaria*), and the Green-Lipped Mussel (*Perna canaliculus*) (Table 5; AmP Collection, 2024; Ren et al., 2020; van der Veer et al., 2006). However, when T_A was calculated from clearance data (Vanderploeg et al., 2010), a much lower estimate was obtained, especially when compared to other species. Figure 6 still shows a general trend of increasing clearance rate with increasing temperature which is similar to Kooijman (2010)'s expectations about temperature response. Although the DEB theory suggests the temperature response of metabolic processes should be identical in an organism (Kooijman, 2010), it is possible that mussel filtration could be determined by a different temperature response relationship than respiration. However, more

evidence from empirical studies is still needed to support this statement. Alternatively, other studies have also calculated different estimates of T_A based on different metabolic processes (van der Veer et al., 2001) or calculation method (Freitas et al., 2011). Which T_A estimate to use can be determined by modelling a physiological process in response to changing temperature and checking against collected data for similar magnitudes (similar to van der Veer et al., 2001).

3.2.4 Maximum surface area-specific ingestion rate ($\{\dot{p}_{Xm}\}$) and maximum surface area-specific searching rate ($\{\dot{F}_m\}$)

For Quagga Mussels, using data collected by Vanderploeg et al. (2010), $\{\dot{p}_{Xm}\}$ was estimated to be 1,000 J d^{-1} cm^{-2} and $\{\dot{F}_m\}$ was estimated to be 150.0 L d^{-1} cm^{-2} (Table 5). Previous estimations of the feeding parameters $\{\dot{p}_{Xm}\}$ and $\{\dot{F}_m\}$ are highly varied depending on the species (Table 5) and the study. Huff (2023) reported an estimate of 103.4 J d^{-1} cm^{-2} for $\{\dot{p}_{Xm}\}$ for Lake Huron and Lake Michigan Quagga Mussels, which is an order of magnitude lower than the estimate in the current study. However, the AmP Collection (2024) estimated $\{\dot{p}_{Xm}\}$ = 850.0 J d^{-1} cm^{-2} for Zebra Mussels and van der Veer et al. (2006) reported a $\{\dot{p}_{Xm}\}$ estimate of 1,200 J d^{-1} cm^{-2} for the Pacific Oyster (*Crassostrea gigas*), both of which are vastly larger than the estimations reported by Huff (2023) but are similar to the estimate in the current study. $\{\dot{F}_m\}$ is also highly varied, ranging from 6.5 to 105.6 L d^{-1} cm^{-2} for different mollusk species (Table 5; AmP Collection, 2024; Lanjouw et al. 2024; Ren et al., 2020); however, the $\{\dot{F}_m\}$ estimate in the current study is slightly higher but relatively close to this previously established range.

As previously demonstrated above (see section 3.1.3), food quality has a large impact on dreissenid mussel clearance rate (Carrick et al., 2023; Vanderploeg et al., 2023), and a similar assumption can be made for most, if not all, mollusk species (Pouil et al., 2021; Rosa et al.,

2018). Therefore, calculations of $\{\dot{p}_{Xm}\}$ and $\{\dot{F}_m\}$ will be largely dependent on the type of food used during experimentation to calculate clearance rates, which may account for the large spread in these parameters both across species and between studies for the same species. For example, Huff (2023) estimated $\{\dot{p}_{Xm}\}$ from a study that used a chlorophyte species as the food source to determine maximum clearance rates. According to the analysis done in the current study in section 3.1.3, chlorophytes are the third most preferred food source, after cryptophytes and diatoms (Carrick et al., 2023; Vanderploeg et al., 2023), which could account for the low $\{\dot{p}_{Xm}\}$ estimation calculated by Huff (2023).

Although numerous dreissenid feeding studies have investigated clearance rates in response to temperature, food type, and turbidity levels (reviewed in Karatayev and Burlakova (2022)), very few feeding studies have taken a systematic approach to quantifying Quagga Mussel clearance rates which include supplying a known food amount with a known energy content, at levels that can either overfeed or starve the mussels. Data collection techniques can complicate interpretation of feeding experiments. The two common practices to measure mussel clearance rate by Vanderploeg et al. (2009) and Vanderploeg et al. (2010) were to take the initial and final water samples from either an undisturbed water column or from a water column that was mixed before and after experimentation. By mixing the water column prior to and after mussel feeding, the final water sample aims to include food that is captured but not processed by the mussels, including pseudo-feces or incompletely digested food, and therefore describes the rate of assimilation by the mussel (Vanderploeg et al., 2009). However, the assimilation rate as described by Vanderploeg et al. (2009) differs from the DEB assimilation rate since the DEB assimilation rate accounts for overhead costs such as processing ingested food to energy and the production of feces (Kooijman, 2010). Thus, since the ingestion rate $\{\dot{p}_{Xm}\}$ was calculated based

on experimental assimilation rates, the current study can only provide a lower estimation of the true-DEB ingestion rate.

With both $\{\dot{p}_{Am}\}$ and $\{\dot{p}_{Xm}\}$ estimated, we were able to calculate the fraction of food energy fixed in reserve (κ_X = 0.09). This parameter helps to convert lab-measured filtration to the reserve energy that is available for the organism to utilize. Although the $\{\dot{p}_{Xm}\}$ estimated for Quagga and Zebra mussels in the current study are higher than other mollusk species, Quagga and Zebra mussels have a lower efficiency in utilizing the food they obtain, which results in a $\{\dot{p}_{Am}\}$ value that is similar to other mollusk species (See Supplementary Material Figure 2).

3.3 Model predictions

3.3.1 Mussel clearance rate predictions

The experimentally informed model parameters predicted the magnitude and trend of the measured clearance rates with success and generally predicted the trend but overpredicted the magnitude of the measured ingestion rate data (Figure 7). Parameter sensitivity was further explored using estimates of $\{\dot{F}_m\}$ and $\{\dot{p}_{Xm}\}$ estimated for other mollusk species in the AmP Collection (2024). For instance, $\{\dot{F}_m\}$ ranges between 10 and 100 L d^{-1} cm^{-2} and $\{\dot{p}_{Xm}\}$ ranges between 10 and 1200 J d^{-1} cm^{-2} for other mollusk species, which accounted for the low model predictions. However, based on the available experimental measurements used in the current study, $\{\dot{F}_m\}$ and $\{\dot{p}_{Xm}\}$ were estimated to be higher for Quagga Mussels than other mollusks (Table 5); therefore, we also explored a high model prediction that accounted for extremely increased estimates of $\{\dot{F}_m\}$ (up to 1,000 L d^{-1} cm^{-2}) and $\{\dot{p}_{Xm}\}$ (up to 1,000 J d^{-1} cm^{-2}). Overall, the high prediction generally predicted measured clearance and ingestion rates similarly to the experimentally informed model with slightly higher estimations in magnitude for ingestion rate

(Figure 7). Alternatively, the low prediction consistently under-predicted both the measured clearance and ingestion rates (Figure 7).

3.3.2 Parameter impacts on mussel growth rate predictions

We simulated Quagga and Zebra mussel growth using varying estimates for T_A and $\{\dot{F}_m\}$ in order to compare the two species (Figure 8). The T_A values calculated for Quagga Mussels in the current study (T_A = 5,970 K; Section 3.2.3) are smaller than estimates for other mollusk species, including the Zebra Mussel (T_A = 8,000 K; AmP Collection, 2024; Table 5). A larger T_A value means that the metabolic process is more sensitive to temperature changes (Kooijman, 2010). Thus, in cold temperatures, an exothermic organism with a lower T_A can maintain a relatively high metabolic rate compared to organisms with higher T_A values when there is abundant food. An exothermic organism with a lower T_A is less sensitive to adverse temperature changes. In our simulation at 3.76°C, we estimated higher growth rates for Quagga Mussels with lower T_A values, than Zebra Mussels with higher T_A values (Figure 8a). Quagga Mussels outgrowing Zebra Mussels in cold temperatures is a pattern that is well supported in the literature (Karatayev et al., 2015; Karatayev et al., 2021; Mills et al., 1996; Rudstam and Gandino, 2020). Additionally, Quagga Mussel success in cold temperatures is also credited as one reason why Quagga Mussels have outcompeted Zebra Mussels in the Great Lakes region (Karatayev et al., 2022; Karatayev et al., 2020). Therefore, the smaller T_A value estimated for Quagga Mussels in the current study, compared to estimates for other mollusk species, may account, in part, for their lower sensitivity to temperature and the invasion success of Quagga Mussels in the cold waters of the Great Lakes.

In contrast to the T_A estimate in the current study, which was lower than Zebra Mussels, we estimated Quagga Mussel ingestion parameters ($\{\dot{F}_m\}$ and $\{\dot{p}_{Xm}\}$) to be higher than most

other mollusk species, including Zebra Mussels (Table 5). These higher ingestion parameters suggest that Quagga Mussels are more efficient at food uptake (Kooijman, 2010). In our simulation (Figure 8b), when a constant and low food concentration of 6 J L^{-1} was supplied, mussels with smaller $\{\dot{F}_m\}$, such as Zebra Mussels ($\{\dot{F}_m\}$ = 50 L cm^{-2}), suffered from shell degrowth while mussels with larger $\{\dot{F}_m\}$, such as Quagga Mussels ($\{\dot{F}_m\}$ = 150 L cm^{-2}), continued to grow. Shell degrowth has been previously observed in Lake Erie when dreissenids were in low food conditions (MacIsaac, 1994). In high food conditions (Figure 8c), the mussel with larger $\{\dot{F}_m\}$ continued to grow larger, but the overall difference compared to the mussel with the lower $\{\dot{F}_m\}$ was smaller than in the low food scenario. This pattern is consistent with observations that Quagga Mussels have higher clearance rates than Zebra Mussels (Tang et al., 2014) and that Quagga Mussels outcompete Zebra Mussels in lower food environments (i.e., profundal zones and oligotrophic environments; Balogh et al., 2023; Karatayev et al., 2011; Metz et al., 2018).

3.4 Future model developments

The DEB parameters estimated in this study provide a framework for future Quagga Mussel modelling efforts. Currently, our model exists in the perpetuation stage (Jakeman et al. 2024), where model revision and improvement are necessary in order to create a fully developed model that can support ongoing decision making and management plans within the Great Lakes and other regions. As additional physiological data become available, the present model can be expanded upon and incorporated into biophysical and biogeochemical models to predict species impacts throughout a whole ecosystem.

While our efforts represent a step forward to create a complete DEB model, additional experiments and physiological data are needed to simulate Quagga Mussel growth, reproduction,

and ecosystem impacts over the full range of conditions encountered by Quagga Mussels in freshwater environments. Van der Veer et al. (2006) discussed the physiological experiments that can be purposefully designed to calculate DEB parameters. For example, a feeding study that takes a systematic approach to quantifying Quagga Mussel clearance rates at different food levels, using consistent and known food concentrations for all levels (similar to Haltiner et al. (2023)), can be used to calculate more robust estimates of $\{\dot{F}_m\}$ and $\{\dot{p}_{Xm}\}$. Using a constant and known food source would eliminate the need to estimate food energy content like in the current study with our EFC and POC conversions. Additionally, investigating Quagga Mussel growth rates under ideal (well-fed) and non-ideal (starving) conditions could provide more robust estimates of shape coefficient (δ_M) and maximum reserve density $[E_m]$ by eliminating the current uncertainty that exists in variables like food density and organism reserve density when using field-collected data (van der Veer et al., 2006). Finally, a study of Quagga Mussel respiration (similar to Tyner et al. (2015) and Alexander and McMahon (2004)) over a range of temperatures until exceeding the critical thermal maxima can provide an estimate of Arrhenius temperature (van der Veer et al., 2006). These additional physiological studies will allow for more robust estimates in the completion of a fully realized Quagga Mussel DEB model.

4. Conclusion

Overall, we utilized existing data from the literature to provide new analyses of Quagga Mussel physiology and estimate key DEB parameters using experimental data (shape coefficient, maximum reserve density, Arrhenius temperature, surface area-specific searching rate, and surface area-specific ingestion rate). We estimated selectivity coefficients for common taxonomic algal groups and sizes and presented a methodology that can be used to calculate the effective food concentration available to mollusks in environments with highly variable plankton

taxonomic structure. Furthermore, we developed an initial calibration of a DEB model to predict Quagga Mussel clearance rates in response to varying environmental conditions and the growth model simulations in the current study highlight the parameters that can explain Quagga Mussels outcompeting Zebra Mussels, particularly in colder environments with low food conditions. While uncertainties in parameter estimates exist, the components of our model hold potential for integration into biogeochemical models to elucidate mussel effects on nutrient cycling and their response to future environmental changes. Additionally, this study provides a framework for other species with insufficient physiological data that aim to utilize the DEB theory and model. Finally, we discuss the well-controlled physiological experiments that will be needed in order to create a fully calibrated Quagga Mussel DEB model that predicts dreissenid growth, clearance rates, and reproductive output within the different lakes of the Great Lakes ecosystem.

Acknowledgements - Funding for this project was provided by the Great Lakes Restoration Initiative (template 2021-1019) to the National Oceanic and Atmospheric Administration Great Lakes Environmental Laboratory. Funding was awarded to Cooperative Institute for Great Lakes Research (CIGLR) through the NOAA Cooperative Agreement with the University of Michigan (NA22OAR4320150). Special thanks to S. Pothoven for access to the Lake Michigan long-term monitoring particulate organic carbon and chlorophyll data, R. Lavaud for assistance with dynamic energy budget theory and execution, and G. Carter for help with organizing the 2018 GLERL feeding experiment data. This manuscript is NOAA GLERL Contribution No. 2072, CIGLR contribution No. 1259, and CMU IGLR contribution No. 214. Any trade, firm, or

product names are used for descriptive purposes and do not imply endorsement by the U.S. Government.

References

Add-my-Pet (AmP) Collection. 2024. Add-my-Pet Collection: Species List. Accessed from: https://www.bio.vu.nl/thb/deb/deblab/add_my_pet/species_list.html

Augustine, S., Jaspers, C., Kooijman, S.A.L.M., Carlotti, F., Poggiale, J.-C., Freitas, V., van der Veer, H., van Walraven, L., 2014. Mechanisms behind the metabolic flexibility of an invasive Comb Jelly. Journal of Sea Research 94, 156-165.

Alexander, J.E., Jr, McMahon, R.F., 2004. Respiratory response to temperature and hypoxia in the Zebra Mussel *Dreissena polymorpha*. Comparative Biochemistry and Physiology Part A 137, 425–434.

Anderson, L.A., 1995. On the hydrogen and oxygen content of marine phytoplankton. Deep Sea Research Part I Oceanographic Research Papers 49, 1675-1680.

Balogh, C., Kobak, J., Faragó, N., Serfőző, Z., 2023. Competition between two congener invaders: Food conditions drive the success of the Quagga over Zebra Mussel in a large shallow lake. Freshwater Biology 68, 1963-1980.

Bierman, V.J., Jr., Kaur, J., DePinto, J.V., Feist, T.J., Dilks, D.W., 2005. Modeling the role of Zebra Mussels in the proliferation of blue-green algae in Saginaw Bay, Lake Huron. Journal of Great Lakes Research 31, 32–55.

Boegehold, A.G., Burtner, A.M., Camilleri, A.C., Carter, G., DenUyl, P., Fanslow, D., Semenyuk, D.F., Godwin, C.M., Gossiaux, D., Johengen, T.H., Kelchner, H., Kitchens, C., Mason, L.A., McCabe, K., Palladino, D., Stuart, D., Vanderploeg, H.A., Errera, R., 2023. Routine monitoring of western Lake Erie to track water quality changes associated with cyanobacterial harmful algal blooms. Earth System Science Data 15, 3853–3868.

Bootsma, H.A., Liao, Q., 2014. Nutrient cycling by dreissenid mussels: Controlling factors and ecosystem response, in: Nalepa, T.F., Schloesser, D.W. (eds.), Quagga and Zebra Mussels: Biology, Impact, and Control. 2nd ed. Taylor & Francis, Cambridge, United Kingdom, pp. 555-574.

Burlakova, L.E., Karatayev, A.Y., Padilla, D.K., 2000. The impact of *Dreissena polymorpha* (PALLAS) invasion on unionid bivalves. International Review of Hydrobiology 85, 529–541.

Carrick, H.J., VanCuren, C., Slate, A., Denef, V.J., Dahal, N., Carter, G., Fanslow, D., Glyshaw, P., Vanderploeg, H.A., 2023. Preferential dreissenid mussel grazing on small plankton can favor cyanobacteria: Experimental evidence from western Lake Erie. Aquatic Ecosystem Health & Management 26, 100-110.

Carter, G.S., Godwin, C.M., Johengen, T.J., Vanderploeg, H.A., Elgin, A.K., Glyshaw, P.W., Carrick, H.J., Dahal, N., Denef, V.J., Fanslow, D.L., Burtner, A.M., Camilleri, A.C., 2023. Impacts of dreissenid mussel growth and activity on phytoplankton and nutrients in Lake Erie's western basin. Aquatic Ecosystem Health & Management 26, 87–99.

Delmott, S.E., Edds, D.R., 2014. Zebra mussel maturation and seasonal gametogenesis in Marion Reservoir, Kansas, USA. BioInvasions Records 3, 247–260.

Elgin, A.K., Glyshaw, P.W., NOAA Great Lakes Environmental Research Laboratory, 2021. Quagga Mussel (*Dreissena rostriformis bugensis*) shell and tissue measurements collected in the Laurentian Great Lakes since 2015. NOAA National Centers for Environmental Information. Dataset. https://doi.org/10.25921/16be-d760. Accessed [February 27, 2024].

Elgin, A.K., Glyshaw, P.W., Carter, G.S., 2023. Western Lake Erie Quagga Mussel growth estimates and evidence of barriers to local population growth. Aquatic Ecosystem Health & Management 26, 120-130.

Elgin, A.K., Glyshaw, P.W., Weidel, B.C., 2022. Depth drives growth dynamics of dreissenid mussels in Lake Ontario. Journal of Great Lakes Research 48, 289-299.

Fahnenstiel, G., Pothoven, S., Vanderploeg, H., Klarer, D., Nalepa, T., Scavia, D., 2010. Recent changes in primary production and phytoplankton in the offshore region of southeastern Lake Michigan. Journal of Great Lakes Research 36, 20-29.

Freitas, V., Lika, K., Witte, J.I., van der Veer, H.W., 2011. Food conditions of the Sand Goby *Pomatoschistus minutus* in shallow waters: An analysis in the context of dynamic energy budget theory. Journal of Sea Research 66, 440-446.

Garrido, M., Philippe, C., Nathalie, M., Béatrice, B., Franck, T., Vanina, P., 2019. Evaluation of FluoroProbe® performance for the phytoplankton-based assessment of the ecological status of Mediterranean coastal lagoons. Environmental Monitoring and Assessment 191, 204-220.

Garton, D.W., McMahon, R., Stoeckmann, A.M., 2014. Limiting environmental factors and competitive interactions between Zebra and Quagga mussels in North America, in: Nalepa, T.F., Schloesser, D.W. (eds.), Quagga and Zebra Mussels: Biology, Impacts, and Control. 2nd ed. Taylor & Francis, Cambridge, United Kingdom, pp. 383-402.

Glyshaw, P.W., Riseng, C.M., Nalepa, T.F., Pothoven, S.A., 2015. Temporal trends in condition and reproduction of Quagga Mussels (*Dreissena rostriformis bugensis*) in southern Lake Michigan. Journal of Great Lakes Research 41, 16–26.

Gobin, J., Lester, N.P., Cottrill, A., Fox, M.G., Dunlop, E.S., 2015. Trends in growth and recruitment of Lake Huron Lake Whitefish during a period of ecosystem change, 1985 to 2012. Journal of Great Lakes Research 41, 405–414.

Griebeler, E.M., Seitz, A., 2007. Effects of increasing temperatures on population dynamics of the Zebra Mussel *Dreissena polymorpha*: Implications from an individual-based model. Oecologia 151, 530–543.

Griffiths, R.W., Schloesser, D.W., Leach, J.H., Kovalak, W.P., 1991. Distribution and dispersal of the Zebra Musse (*Dreissena poIymorpha*) in the Great Lakes region. Canadian Journal of Fisheries and Aquatic Sciences 48, 1381 -1388.

Haltiner, L., Rossbacher, S., Alexander, J., Dennis, S.R., Spaak, P., 2023. Life in a changing environment: Dreissenids' feeding response to different temperature. Hydrobiologia 850, 4879–4890.

Hebert, P.D.N., Muncaster, B.W., Mackie, G.L., 1989. Ecological and genetic studies on *Dreissena polymorpha* (Pallas): A new mollusc in the Great Lakes. Canadian Journal of Fisheries and Aquatic Sciences 46, 1587-1591.

Hedges, J.I., Stern, J.H., 1984. Carbon and nitrogen determinations of carbonate-containing solids. Limnology and Oceanography 29, 663-666.

Holeck, K.T., Rudstam, L.G., Hotaling, C., Lemon, D., Pearsall, W., Lantry, J., Connerton, M., Legard, C., LePan, S., Biesinger, Z., Lantry, B.F., Weidel, B.C., 2019. 2018 Status of the Lake Ontario lower trophic levels, 2018 Annual report Bureau of Fisheries Lake Ontario Unit and St. Lawrence River Unit to the Great Lakes Fishery Commission's Lake Ontario Committee. U.S. Geological Survey, p. 28 p.

Horst, G.P., Sarnelle, O., White, J.D., Hamilton, S.K., Kaul, R.B., Bressie, J.D., 2014. Nitrogen availability increases the toxin quota of a harmful cyanobacterium, *Microcystis aeruginosa*. Water Research 54, 188-198.

Hoyle, J.A., Bowlby, J.N., Morrison, B.J., 2008. Lake Whitefish and Walleye population responses to dreissenid mussel invasion in eastern Lake Ontario. Aquatic Ecosystem Health & Management 11, 403-411.

Huff, A., 2023. Dreissenid-mediated energy and nutrient cycling in profundal regions of the Laurentian Great Lakes. University of Minnesota, p. 160.

Jakeman, A.J., Elsawah, S., Wang, H.-H., Hamilton, S.H., Melsen, L., Grimm, V., 2024. Towards normalizing good practice across the whole modeling cycle: Its instrumentation and future research topics. Socio-Environmental Systems Modelling 6, 18755.

Juhel, G., Culloty, S.C., O'Riordan, R.M., O'Connor, J., De Faoite, L., Mcnamara, R., 2003. A histological study of the gametogenic cycle of the freshwater mussel *Dreissena polymorpha* (Pallas, 1771) in Lough Derg, Ireland. Journal of Molluscan Studies 69, 365–373.

Karatayev, A.Y., Burlakova, L.E., 2022. What we know and don't know about the invasive Zebra (*Dreissena polymorpha*) and Quagga (*Dreissena rostriformis bugensis*) Mussels. Hydrobiologia, 1-74.

Karatayev, A.Y., Burlakova, L.E., Mehler, K., Elgin, A.K., Rudstam, L.G., Watkins, J.M., Wick, M., 2022. *Dreissena* in Lake Ontario 30 years post-invasion. Journal of Great Lakes Research 48, 264–273.

Karatayev, A. Y., Burlakova, L. E., Mehler, S. E., Elgin, A. K., Nalepa, T. F., 2020. Lake Huron benthos survey cooperative science and monitoring initiative 2017. Buffalo, New York, USA.

Karatayev, A.Y., Burlakova, L.E., Padilla, D.K., 2006. Growth rate and longevity of *Dreissena polymorpha* (PALLAS): A review and recommendations for future study. Journal of Shellfish Research 25, 23-32.

Karatayev, A.Y., Burlakova, L.E., Padilla, D.K., 2015. Zebra versus Quagga Mussels: A review of their spread, population dynamics, and ecosystem impacts. Hydrobiologia 746, 97–112.

Karatayev, A.Y., Karatayev, V.A., Burlakova, L.E., Mehler, K., Rowe, M.D., Elgin, A.K., Nalepa, T.F., 2021. Lake morphometry determines *Dreissena* invasion dynamics. Biological Invasions, 1-28.

Karatayev, A.Y., Karatayev, V.A., Burlakova, L.E., Rowe, M.D., Mehler, K., Clapsadl, M.D., 2018. Food depletion regulates the demography of invasive dreissenid mussels in a stratified lake. Limnology and Oceanography 63, 2065–2079.

Karatayev, A.Y., Mastitsky, S.E., Padilla, D.K., Burlakova, L.E., Hajduk, M.M., 2011. Differences in growth and survivorship of Zebra and Quagga Mussels: Size matters. Hydrobiologia, 183–194.

Kemp, J.S., Aldridge, D.C., 2018. Comparative functional responses to explain the impact of sympatric invasive bivalves (*Dreissena* spp.) under different thermal regimes. Journal of Molluscan Studies 84, 175–181.

Kooijman, S.A.L.M., 2010. Dynamic Energy Budget Theory for Metabolic Organisation, 3rd ed. Cambridge University Press, Cambridge.

Kooijman, S.A.L.M., 2020. The standard dynamic energy budget model has no plausible alternatives. Ecological Modelling 428, 109106.

Kooijman, S.A.L.M., 2023. Comments on Dynamic Energy Budget theory for Metabolic Organisation. 343 pp.

Lavaud, R., Marn, N., Domingos, T., Filgueira, R., Lika, K., Rakel, K., Klanjšček, T., 2025. Metabolic organization across scales of space and time. Ecological Modelling 500, 110951.

Lanjouw, M., Jansen, H.M., van der Meer, J., 2024. Exploring aquaculture related traits of the Grooved Carpet Shell (*Ruditapes decussatus*) in relation to other bivalve species using dynamic energy budget theory. Ecological Modelling 498, 110883.

Lika, K., Kearney, M.R., Freitas, V., van der Veer, H.W., van der Meer, J., Wijsman, J.W.M., Pecquerie, L., Kooijman, S.A.L.M., 2011a. The "covariation method" for estimating the parameters of the standard dynamic energy budget model I: Philosophy and approach. Journal of Sea Research 66, 270–277.

Lika, K., Kearney, M.R., Kooijman, S.A.L.M., 2011b. The "covariation method" for estimating the parameters of the standard dynamic energy budget model II: Properties and preliminary patterns. Journal of Sea Research 66, 278–288.

Lika, K., Kooijman, S.A.L.M., 2011. The comparative topology of energy allocation in budget models. Journal of Sea Research 66, 381-391.

Limburg, K.E., Luzadis, V.A., Ramsey, M., Schulz, K.L., Mayer, C.M., 2010. The good, the bad, and the algae: Perceiving ecosystem services and disservices generated by Zebra and Quagga Mussels. Journal of Great Lakes Research 36, 86–92.

MacIsaac, H.J., 1994. Comparative growth and survival of *Dreissena polymorpha* and *Dreissena bugensis*, exotic molluscs introduced to the Great Lakes. Journal of Great Lakes Research 20, 783-790.

Madenjian, C.P., 1995. Removal of algae by the Zebra Mussel (*Dreissena polymorpha*) population in western Lake Erie: A bioenergetics approach. Canadian Journal of Fisheries and Aquatic Sciences 52, 381-390.

Madenjian, C.P., Bunnell, D.B., Warner, D.M., Pothoven, S.A., Fahnenstiel, G.L., Nalepa, T.F., Vanderploeg, H.A., Tsehaye, I., Claramunt, R.M., Clark, R.D., Jr., 2015. Changes in the Lake Michigan food web following dreissenid mussel invasions: A synthesis. Journal of Great Lakes Research 41, 217–231.

Marn, N., Hudina, S., Haberle, I., Dobrovic, A., Klanjscek, T., 2022. Physiological performance of native and invasive crayfish species in a changing environment: Insights from dynamic energy budget models. Conservation Physiology 10, coac031.

Marques, G.M., Augustine, S., Lika, K., Pecquerie, L., Domingos, T., Kooijman, S.A.L.M., 2018. The AmP project: Comparing species on the basis of dynamic energy budget parameters. PloS Computational Biology 14, e1006100.

Metz, O., Temmen, A., von Oheimb, K.C.M., Albrecht, C., Schubert, P., Wilke, T., 2018. Invader vs. invader: Intra- and interspecific competition mechanisms in Zebra and Quagga Mussels. Aquatic Invasions 13, 473–480.

Mills, E.L., Dermott, R.M., Roseman, E.F., Dustin, D., Mellina, E., Conn, D.B., Spidle, A.P., 1993. Colonization, ecology, and population structure of the "Quagga" Mussel (Bivalvia: Dreissenidae) in the lower Great Lakes. Canadian Journal of Fisheries and Aquatic Sciences 50, 2305-2314.

Mills, E.L., Rosenberg, G., Spidle, A.P., Ludyanskiy, M., Pligin, Y., May, B., 1996. A review of the biology and ecology of the Quagga Mussel (*Dreissena bugensis*), a second species of freshwater dreissenid introduced to North America. American Zoologist 36, 271-286.

National Oceanic and Atmospheric Administration Great Lakes Environmental Research Laboratory (NOAA GLERL), 2024. Water Quality and Buoy Data. https://www.glerl.noaa.gov/res/HABs_and_Hypoxia/habsMon.html Accessed [July 18, 2023].

Nepal, V., Fabrizio, M.C., Lavaud, R., van der Meer, J., 2024. Bioenergetic strategies contributing to the invasion success of Blue Catfish. Ecological Modelling 496, 110830.

Pothoven, S.A., Vanderploeg, H.A., 2020. Seasonal patterns for Secchi depth, chlorophyll *a*, total phosphorus, and nutrient limitation differ between nearshore and offshore in Lake Michigan. Journal of Great Lakes Research 46, 519–527.

Pouil, S., Hills, A., Mathews, T.J., 2021. The effects of food quantity, light, and temperature on clearance rates in freshwater bivalves (Cyrenidae and Unionidae). Hydrobiologia 848, 675-689.

Prescott, T.H., Claudi, R., Prescott, K.L., 2014. Impact of dreissenid mussels on the infrastructure of dams and hydroelectric power plants, in: Nalepa, T.F., Schloesser, D.W. (eds.), Quagga and Zebra Mussels: Biology, Impact, and Control. 2nd ed. Taylor & Francis, Cambridge, United Kingdom, pp. 243-257.

Ram, J.L., Karim, A.S., Banno, F., Kashian, D.R., 2012. Invading the invaders: Reproductive and other mechanisms mediating the displacement of Zebra Mussels by Quagga Mussels. Invertebrate Reproduction & Development 56, 21-32.

Redfield, A.C., 1933. On the proportions of organic derivatives in sea water and their relation to the composition of plankton. James Johnstone Memorial Volume, 176-192.

Ren, J.S., Ragg, N.L.C., Cummings, V.J., Zhang, J., 2020. Ocean acidification and dynamic energy budget models: Parameterisation and simulations for the Green-Lipped Mussel. Ecological Modelling 426, 109069.

Ricciardi, A., Bourget, E., 1998. Weight-to-weight conversion factors for marine benthic macroinvertebrates. Marine Ecology Progress Series 163, 245-251.

Rosa, M., Ward, J.E., Shumway, S.E., 2018. Selective capture and ingestion of particles by suspension-feeding bivalve molluscs: A review. Journal of Shellfish Research 37, 727-746.

Rowe, M.D., Anderson, E.J., Vanderploeg, H.A., Pothoven, S.A., Elgin, A.K., Wang, J., Yousef, F., 2017. Influence of invasive Quagga Mussels, phosphorus loads, and climate on spatial and temporal patterns of productivity in Lake Michigan: A biophysical modeling study. Limnology and Oceanography 62, 2629–2649.

Rudstam, L.G., Gandino, C.J., 2020. Zebra or Quagga Mussel dominance depends on trade-offs between growth and defense— Field support from Onondaga Lake, NY. PLoS ONE 15, e0235387.

Sarà, G., Palmeri, V., Montalto, V., Rinaldi, A., Widdows, J., 2013. Parameterisation of bivalve functional traits for mechanistic eco-physiological dynamic energy budget (DEB) models. Marine Ecology Progress Series 480, 99–117.

Saraiva, S., van der Meer, J., Kooijman, S.A.L.M., Sousa, T., 2011. DEB parameters estimation for *Mytilus edulis*. Journal of Sea Research 66, 289–296.

Saraiva, S., van der Meer, J., Kooijman, S.A.L.M., Witbaard, R., Philippart, C.J.M., Hippler, D., Parker, R., 2012. Validation of a dynamic energy budget (DEB) model for the Blue Mussel *Mytilus edulis*. Marine Ecology Progress Series 463, 141–158.

Schneider, D.W., 1992. A bioenergetics model of Zebra Mussel, *Dreissena polymorpha*, growth in the Great Lakes. Canadian Journal of Fisheries and Aquatic Sciences 49, 1406-1416.

Speziale, B.J., Schreiner, S.P., Giammatteo, P.A., Schindler, J.E., 1984. Comparison of N,N-Dimethylformamide, Dimethyl Sulfoxide, and acetone for extraction of phytoplankton chlorophyll. Canadian Journal of Fisheries and Aquatic Sciences 41, 1519-1522.

Spidle, A.P., Mills, E.L., May, B., 1995. Limits to tolerance of temperature and salinity in the Quagga Mussel (*Dreissena bugensis*) and Zebra Mussel (*Dreissena polymorpha*). Canadian Journal of Fisheries and Aquatic Sciences 52, 2108-2119.

Stadig, M.H., Collingsworth, P.D., Lesht, B.M., Höök, T.O., 2020. Spatially heterogeneous trends in nearshore and offshore chlorophyll *a* concentrations in lakes Michigan and Huron (1998–2013). Freshwater Biology 65, 366–378.

Strayer, D.L., Smith, L.C., Hunter, D.C., 1998. Effects of the Zebra Mussel (*Dreissena polymorpha*) invasion on the macrobenthos of the freshwater tidal Hudson River. Canadian Journal of Zoology 76, 419–425.

Sturtevant, R.A., Mason, D.M., Rutherford, E.S., Elgin, A., Lower, E., Martinez, F., 2019. Recent history of nonindigenous species in the Laurentian Great Lakes; An update to Mills et al., 1993 (25 years later). Journal of Great Lakes Research 45, 1011–1035.

Tang, H., Vanderploeg, H.A., Johengen, T.H., Liebig, J.R., 2014. Quagga Mussel (*Dreissena rostriformis bugensis*) selective feeding of phytoplankton in Saginaw Bay. Journal of Great Lakes Research 40, 83–94.

Tyner, E.H., Bootsma, H.A., Lafrancois, B.M., 2015. Dreissenid metabolism and ecosystem-scale effects as revealed by oxygen consumption. Journal of Great Lakes Research 41, 27–37.

van der Meer, J., 2006. An introduction to dynamic energy budget (DEB) models with special emphasis on parameter estimation. Journal of Sea Research 56, 85–102.

van der Veer, H.W., Cardoso, J.F.M.F., van der Meer, J., 2006. The estimation of DEB parameters for various Northeast Atlantic bivalve species. Journal of Sea Research 56, 107–124.

van der Veer, H.W., Kooijman, S.A.L.M., van der Meer, J., 2001. Intra- and interspecies comparison of energy flow in North Atlantic flatfish species by means of dynamic energy budgets. Journal of Sea Research 45, 303-320.

Vanderploeg, H.A., Glyshaw, P.W., Carrick, H.J., Carter, G.S., Dahal, N., Denef, V.J., Fanslow, D.L., Godwin, C.M., 2023. Seasonal interactions between Quagga Mussel grazing and phytoplankton in western Lake Erie: The view from different measuring technologies. Aquatic Ecosystem Health & Management 26, 111-119.

Vanderploeg, H.A., Johengen, T.H., Liebig, J.R., 2009. Feedback between Zebra Mussel selective feeding and algal composition affects mussel condition: Did the regime changer pay a price for its success? Freshwater Biology 54, 47–63.

Vanderploeg, H.A., Liebig, J.R., Carmichael, W.W., Agy, M.A., Johengen, T.H., Fahnenstiel, G.L., Nalepa, T.F., 2001. Zebra Mussel (*Dreissena polymorpha*) selective filtration promoted toxic *Microcystis* blooms in Saginaw Bay (Lake Huron) and Lake Erie. Canadian Journal of Fisheries and Aquatic Sciences 58, 1208–1221.

Vanderploeg, H.A., Liebig, J.R., Nalepa, T.F., Fahnenstiel, G.L., Pothoven, S.A., 2010. *Dreissena* and the disappearance of the spring phytoplankton bloom in Lake Michigan. Journal of Great Lakes Research 36, 50–59.

Vanderploeg, H.A., Sarnelle, O., Liebig, J.R., Morehead, N.R., Robinson, S.D., Johengen, T.H., Horst, G.P., 2017. Seston quality drives feeding, stoichiometry and excretion of Zebra Mussels. Freshwater Biology 62, 664–680.

Vanderploeg, H.A., Scavia, D., Liebig, J.R., 1984. Feeding rate of *Diaptomus sicilis* and its relation to selectivity and effective food concentration in algal mixtures and in Lake Michigan. Journal of Plankton Research 6, 919-941.

Vanderploeg, H.A., Wilson, A.E., Johengen, T.H., Bressie, J.D., Sarnelle, O., Liebig, J.R., Robinson, S.D., Horst, G.P., 2014. Role of selective grazing by dreissenid mussels in promoting toxic microcystis blooms and other changes in phytoplankton composition in the Great Lakes, in: Nalepa, T.F., Schloesser, D.W. (eds.), Quagga and Zebra Mussels: Biology, Impacts and Control. 2nd ed. Taylor & Francis, Cambridge, United Kingdom, pp. 509-523.

White, J.D., Sarnelle, O., 2014. Size-structured vulnerability of the colonial cyanobacterium, *Microcystis aeruginosa*, to grazing by Zebra Mussels (*Dreissena polymorpha*). Freshwater Biology 59, 514–525.

Zalusky, J.A., 2021. Starvation in the depths: How Quagga Mussels persist in the most challenging habitat of the Laurentian Great Lakes. University of Minnesota, p. 105.

Tables and Figures

Table 1. Energy density and elemental composition (C, H, O, N, and P) by moles and by mass from different sources. Elemental composition of Quagga Mussel (*Dreissena rostriformis bugensis*) and Zebra Mussel (*D. polymorpha*) tissues from the Great Lakes region collected by Carter et al. (2023) and Vanderploeg et al. (2017), respectively. Elemental composition of marine phytoplankton recognized as the Redfield ratio (Redfield, 1958) and improved by Anderson (1995). Energy density and elemental composition according to the standard dynamic energy budget (DEB) model (Kooijman, 2010). For experimental datasets, the value is followed by standard error.

Organism	C	H	N	O	P	Energy Density (J C-mol^{-1})	Source
Chemical indices per 1 C-mol of dry tissue							
Quagga Mussel	1	-	0.21 ± 0.001	-	0.0054 ± 0.0002	-	Carter et al. (2023)
Zebra Mussel	1	-	0.21 ± 0.01	-	0.0078 ± 0.0006	-	Vanderploeg et al. (2017)
Marine Phytoplankton	1	1.7	0.15	0.4	0.0094	-	Redfield (1958) & Anderson (1995)
Food	1	1.8	0.15	0.5	-	525,000	Kooijman (2010)
Structure	1	1.8	0.15	0.5	-	500,000	Kooijman (2010)
Reserve	1	1.8	0.15	0.5	-	550,000	Kooijman (2010)
Feces	1	1.8	0.15	0.5	-	480,000	Kooijman (2010)
Elemental weight in dry tissue weight (mg/mg)							
Quagga Mussel	0.46 ± 0.005	-	0.11 ± 0.001	-	0.006 ± 0.0003	-	Carter et al. (2023)

Zebra Mussel	0.50 ± 0.009	-	0.12 ± 0.006	-	0.010 ± 0.0007	-	Vanderploeg et al. (2017)
Marine Phytoplankton	0.54	0.07	0.09	0.28	0.013	-	Redfield (1958) & Anderson (1995)
Random microorganism	0.50	0.09	0.08	0.33	-	-	Kooijman (2010)

1102

Table 2. Summary of the parameter values (surface area-specific searching rate ($\{\dot{F}_m\}$), surface area-specific ingestion rate ($\{\dot{p}_{Xm}\}$), and half saturation coefficient (K)) used to create the experimentally-informed, low, and high ingestion rate model predictions.

	$\{\dot{F}_m\}$ (L d^{-1} cm^{-2})	$\{\dot{p}_{Xm}\}$ (J d^{-1} cm^{-2})	K (J L^{-1})
Low	100	100	1
Experimentally-Informed, Vanderploeg et al. (2010)	150	1000	6.67
High	1000	1000	1

Table 3. Type II standard major axis regression (with intercept = 0, degrees of freedom = 1) for each independent (idp) - dependent (dpd) variable measuring different Quagga Mussel (*Dreissena rostriformis bugensis*) weights. Slopes are presented with ± standard error. Abbreviations follow: tissue dry weight (TDW), tissue ash free dry weight (AFDW), tissue wet weight (TWW), and shell weight (SW).

idp [mg]	dpd [mg]	Slope ± SE	r^2	n	Conversion Formula
TDW	AFDW	$0.862 \pm 1.04 * 10^{-3}$	0.996	3039	AFDW = 0.862 * TDW TDW = AFDW / 0.862
TWW	AFDW	$0.0386 \pm 6.69 * 10^{-5}$	0.867	249	AFDW = 0.0386 * TWW TWW = AFDW / 0.0386
SW	AFDW	$0.0763 \pm 5.72 * 10^{-5}$	0.903	3002	AFDW = 0.0763 * SW SW = 0.0763 / AFDW

Table 4. Selectivity coefficients (w_i') ± standard error calculated from Quagga Mussel (*Dreissena rostriformis bugensis*) clearance rate data collected using microscopy during the 2018 feeding experiments as described by Carrick et al. (2023).

Classification Method	Feeding Type	Abbreviation	Explanation	wi'
Size Class	Heterotrophic	Hmicro	20 – 200 μm	0.60 ± 0.20
		Hnano	2 – 20 μm	0.90 ± 0.18
	Phototrophic	Pmicro	20 – 200 μm	0.54 ± 0.12
		Pnano	2 – 20 μm	1.00 ± 0.00
		Ppico	0.2 – 2 μm	0.28 ± 0.10
Taxon Groups	Phototrophic	Bac	Bacillariophyta	0.83 ± 0.42
		Chl	Chlorophyta	0.16 ± 0.31
		Cry	Cryptophyta	1.00 ± 0.00
		Cyn	Cyanobacteria	0.10 ± 0.24
		Pra	Prasinomondida	0.95 ± 0.19
	Heterotrophic	Cil	Ciliophora	0.50 ± 0.14
		Chr	Chrysomonadida	0.74 ± 0.16
		Din	Dinoflagellida	1.52 ± 1.39

Table 5. Estimates of Dynamic Energy Budget model parameters for Quagga Mussels (*Dreissena rostriformis bugensis*), Zebra Mussels (*D. polymorpha*), and other mollusk species.

Symbol	Description	Unit	Value	Species	Reference
T_A	Arrhenius temperature	K	5969.9 ± 802.0	*D. r. bugensis*	This study (Tyner et al., 2015)
			2552.0 ± 1266.1	*D. r. bugensis*	This study (Vanderploeg et al., 2010)
			8000	*D. polymorpha*	AmP Collection (2024)
			7051	*Mya arenaria*	AmP Collection (2024)
			8000	*Corbicula fluminea*	AmP Collection (2024)
			8000	*Elliptio complanata*	AmP Collection (2024)
			8000	*Obliquaria reflexa*	AmP Collection (2024)
			8000	*Truncilla truncata*	AmP Collection (2024)
			7022	*Mytilus edulis*	van der Veer et al. (2006)
			4559	*Crassostrea virginica*	AmP Collection (2024)
			5300	*Perna canaliculus*	Ren et al. (2020)
			3459	*Ruditapes decussatus*	Lanjouw et al. (2024)
δ_M	Shape coefficient	-	0.225 ± 0.1	*D. r. bugensis*	This study (Elgin and Glyshaw, 2021)
			0.34	*D. r. bugensis*	Huff (2023)

			0.345	*D. polymorpha*	AmP Collection (2024)
			0.286	*M. arenaria*	AmP Collection (2024)
			0.642	*C. fluminea*	AmP Collection (2024)
			0.277	*E. complanata*	AmP Collection (2024)
			0.303	*O. reflexa*	AmP Collection (2024)
			0.256	*T. truncata*	AmP Collection (2024)
			0.297	*M. edulis*	Saraiva et al. (2011)
			0.25	*P. canaliculus*	Ren et al. (2020)
			0.5864	*R. decussatus*	Lanjouw et al. (2024)
$[E_M]$	Maximum reserve density	J cm^{-3}	4516.7 ± 33.6	*D. r. bugensis*	This study (Elgin and Glyshaw, 2021)
			3520	*D. r. bugensis*	Huff (2023)
			5200	*D. polymorpha*	AmP Collection (2024)
			2190	*M. edulis*	van der Veer et al. (2006)
			2805	*E. complanata*	AmP Collection (2024)
			593	*O. reflexa*	AmP Collection (2024)
			1212	*T. truncata*	AmP Collection (2024)
			2080	*Cerastoderma edule*	van der Veer et al. (2006)

			2340	*Crassostrea gigas*	van der Veer et al. (2006)
			4835	*P. canaliculus*	Ren et al. (2020)
K	Half saturation coefficient	J L^{-1}	6.67	*D. polymorpha*	This study (Vanderploeg et al., 2009)
			17.60	*D. polymorpha*	AmP Collection (2024)
			0.11	*M. edulis*	AmP Collection (2024)
			2.47	*E. complanata*	AmP Collection (2024)
			2.29	*O. reflexa*	AmP Collection (2024)
			4.54	*T. truncata*	AmP Collection (2024)
			0.45	*C. virginica*	AmP Collection (2024)
		mmol C m^{-3}	33.53	*D. r. bugensis*	Huff (2023)
$\{\dot{F}_m\}$	Maximum surface area-specific searching rate	L d^{-1} cm^{-2}	150.0	*D. r. bugensis*	This study (Vanderploeg et al., 2010)
			64.6	*D. polymorpha*	This study (Vanderploeg et al., 2009)
			48.2	*D. polymorpha*	AmP Collection (2024)
			6.5	*M. arenaria*	AmP Collection (2024)
			6.5	*C. fluminea*	AmP Collection (2024)
			105.6	*M. edulis*	AmP Collection (2024)

			6.5	*E. complanata*	AmP Collection (2024)
			6.5	*O. reflexa*	AmP Collection (2024)
			6.5	*T. truncata*	AmP Collection (2024)
			32.0	*C. virginica*	AmP Collection (2024)
$\{\dot{p}_{Xm}\}$	Maximum surface area-specific ingestion rate	J d^{-1} cm^{-2}	1000	*D. r. bugensis*	This study (Vanderploeg et al., 2010)
			103.4	*D. r. bugensis*	Huff (2023)
			55.8	*D. polymorpha*	This study (Vanderploeg et al., 2009)
			850.0	*D. polymorpha*	AmP Collection (2024)
			11.7	*M. edulis*	AmP Collection (2024)
			16.0	*E. complanata*	AmP Collection (2024)
			14.9	*O. reflexa*	AmP Collection (2024)
			29.5	*T. truncata*	AmP Collection (2024)
			14.3	*C. virginica*	AmP Collection (2024)
			1200	*C. gigas*	van der Veer et al. (2006)
$\{\dot{p}_{Am}\}$	Maximum surface area-specific assimilation rate	J d^{-1} cm^{-2}	90.33	*D. r. bugensis*	This study
			78.2	*D. r. bugensis*	Huff (2023)

			85.0	*D. polymorpha*	AmP Collection (2024)
			3.2	*M. arenaria*	AmP Collection (2024)
			54.6	*C. fluminea*	AmP Collection (2024)
			11.1	*M. edulis*	AmP Collection (2024)
			12.8	*E. complanata*	AmP Collection (2024)
			11.9	*O. reflexa*	AmP Collection (2024)
			23.6	*T. truncata*	AmP Collection (2024)
			11.4	*C. virginica*	AmP Collection (2024)
			109.2	*P. canaliculus*	Ren et al. (2020)
$[\dot{p}_M]$	Volume-specific somatic maintenance rate	J d^{-1} cm^{-3}	154.2	*D. r. bugensis*	This study
			96.0	*D. polymorpha*	AmP Collection (2024)
			8.4	*M. arenaria*	AmP Collection (2024)
			18.0	*C. fluminea*	AmP Collection (2024)
			2.6	*M. edulis*	AmP Collection (2024)
			6.1	*E. complanata*	AmP Collection (2024)
			7.4	*O. reflexa*	AmP Collection (2024)
			12.9	*T. truncata*	AmP Collection (2024)

1119

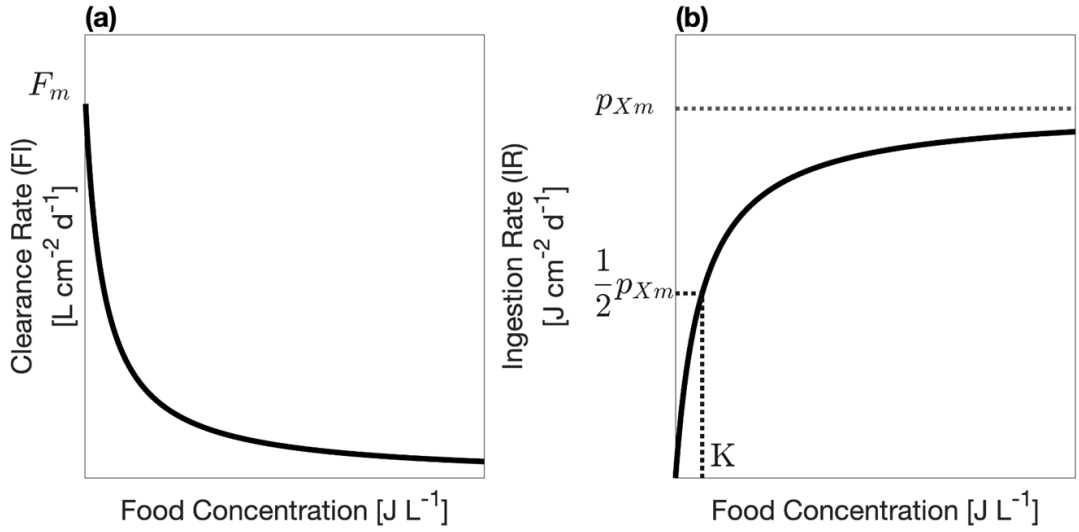

1120

1121 Figure 1. Expected patterns for clearance rate (a) and ingestion rate (b) from a typical mussel
1122 (e.g., *Dreissena* spp.) feeding experiment testing clearance rate at different food levels while
1123 maintaining constant temperature and mussel size.
1124

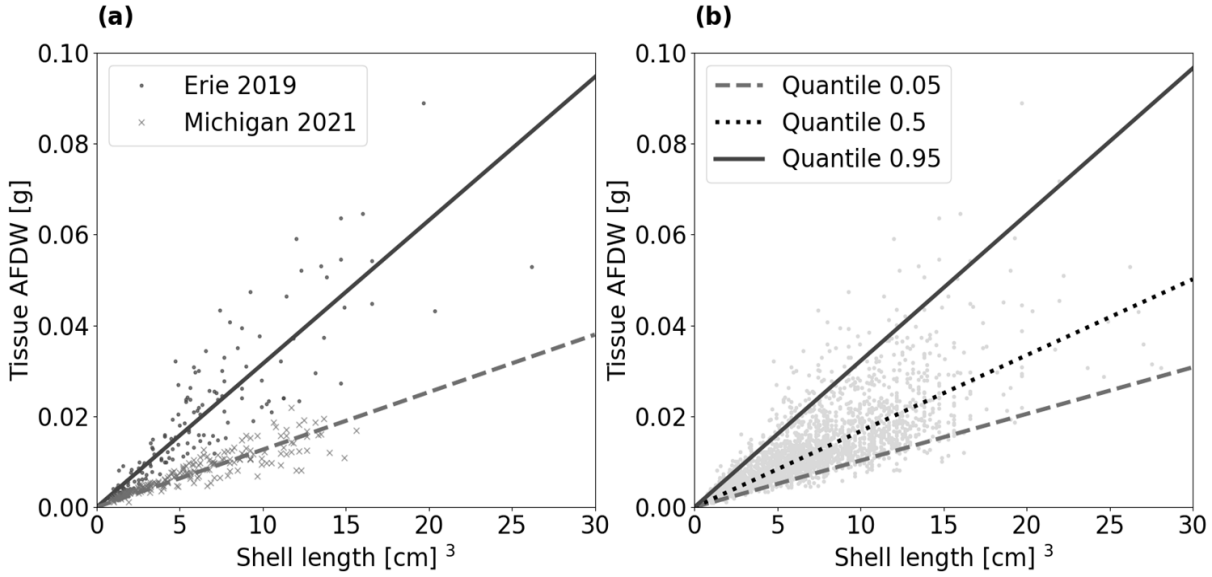

Figure 2. Regressions of Quagga Mussel (*Dreissena rostriformis bugensis*) tissue ash-free dry weight (g AFDW) on shell length cubed (cm^3) for well-fed mussels (solid line) and starved (dashed line) mussels. (a) Mussel length and weight data comes from shallow (<30 m) Lake Erie 2019 sites where mussels are assumed to be well fed and from mid-depth (30-90 m) Lake Michigan 2021 sites where mussels are assumed to be starving. (b) Mussel length and weight data comes from all sites in Lake Ontario (2018, 2023), Erie (2019), Huron (2017, 2022), and Michigan (2015, 2021) (light gray points). The 0.5 quantile (dotted line) represents the median values, the 0.95 quantile represents well-fed mussels, and the 0.05 quantile represents starving mussels. Data source: Elgin and Glyshaw (2021).

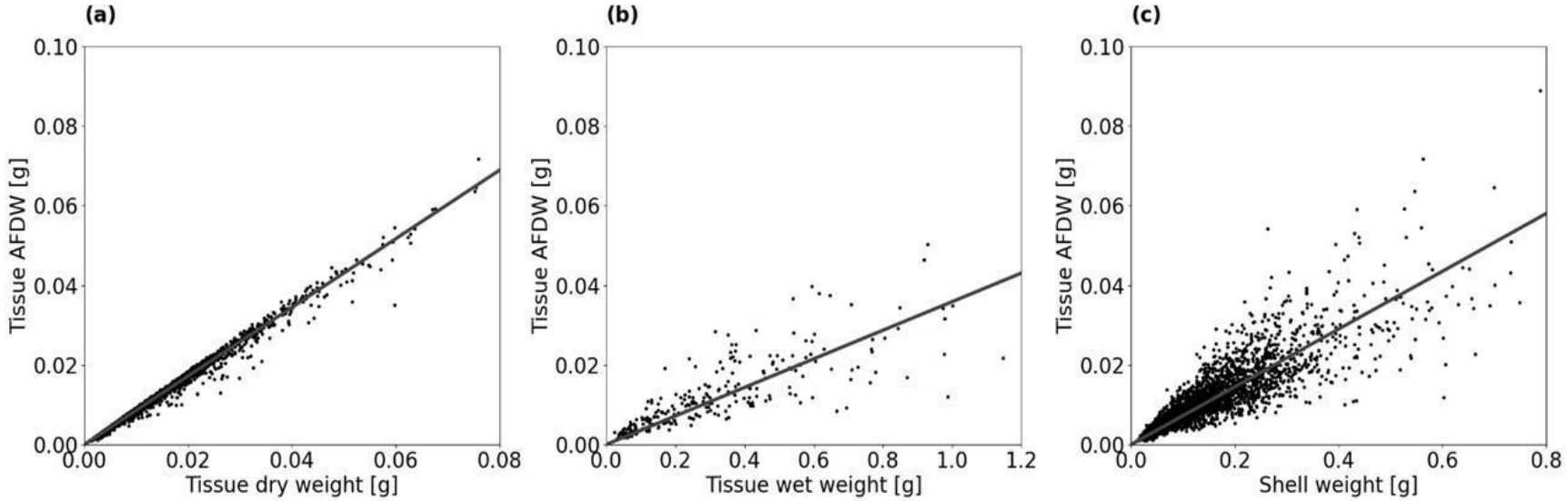

Figure 3. Observations and standard major axis regressions between (a) Quagga Mussel (*Dreissena rostriformis bugensis*) tissue dry weight and tissue ash free dry weight, (b) Quagga Mussel wet weight (whole mussel wet weight - shell weight) and tissue ash free dry weight, and (c) Quagga Mussel shell weight (g) and tissue ash free dry weight. Data collected from Lake Ontario (2018, 2023), Erie (2019), Huron (2017, 2022), and Michigan (2015, 2021) and represented as black dots. Data source: Elgin and Glyshaw (2021).

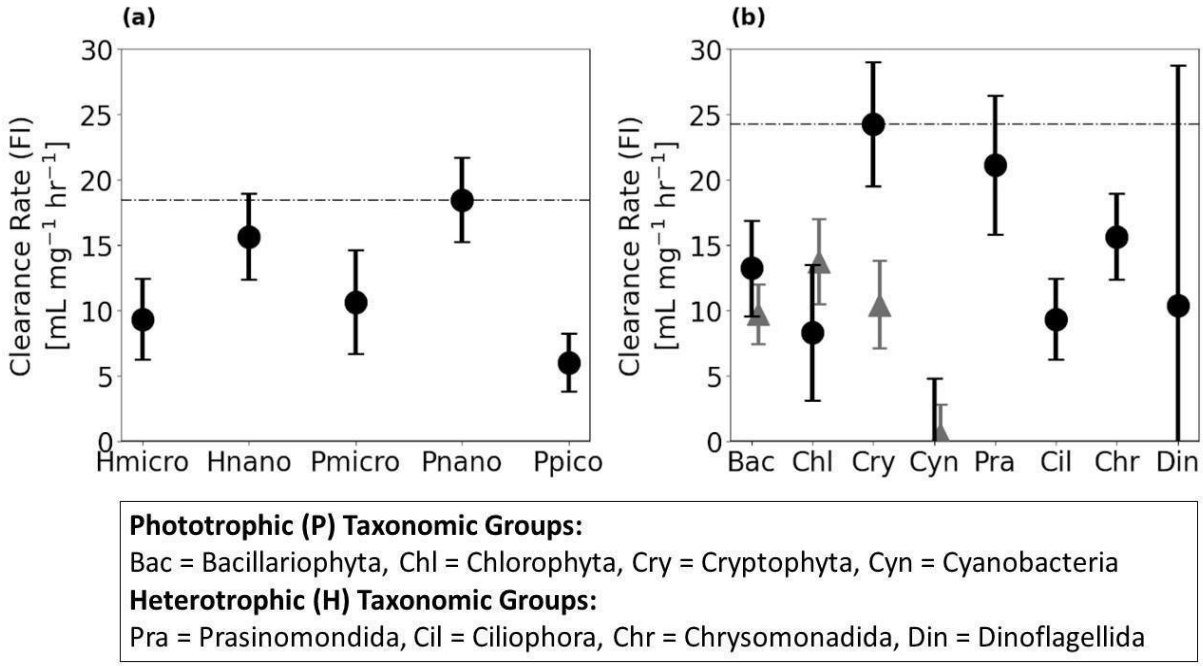

Figure 4. Quagga Mussel (*Dreissena rostriformis bugensis*) clearance rates (FI) for (a) different chlorophyll size fractions and (b) for different taxonomic groups. Microscopy data (black circles) are from Carrick et al. (2023) and FluoroProbe data (gray triangles) are from Vanderploeg et al. (2023). The central point represents the mean and whiskers represent standard error. The horizontal dot-dashed line represents the clearance rate of the reference (or anchored) food source. Mean mussel size was 19.5 mm. Temperature conditions were corrected using Eq. 10.

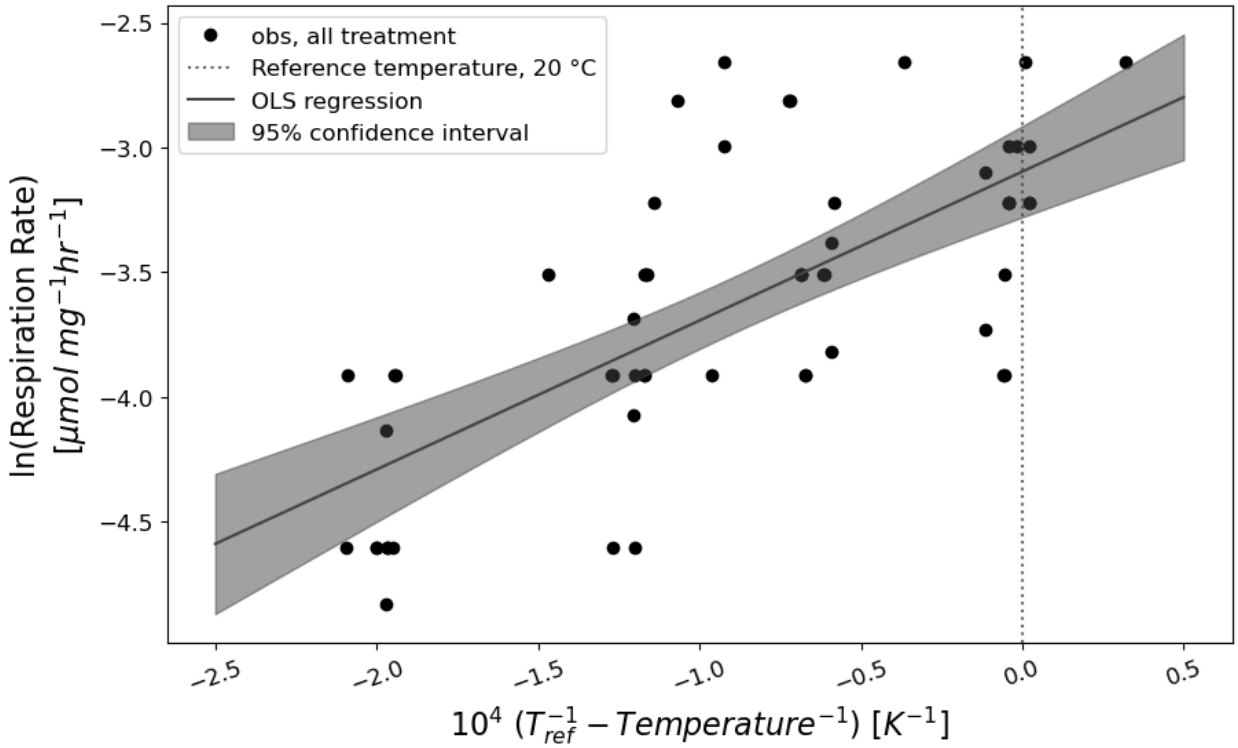

Figure 5. Experimental Quagga Mussel (*Dreissena rostriformis bugensis*) respiration rates (natural log-transformed) by inverse reference temperature minus inverse temperature of measurement. Data source: Tyner et al. (2015).

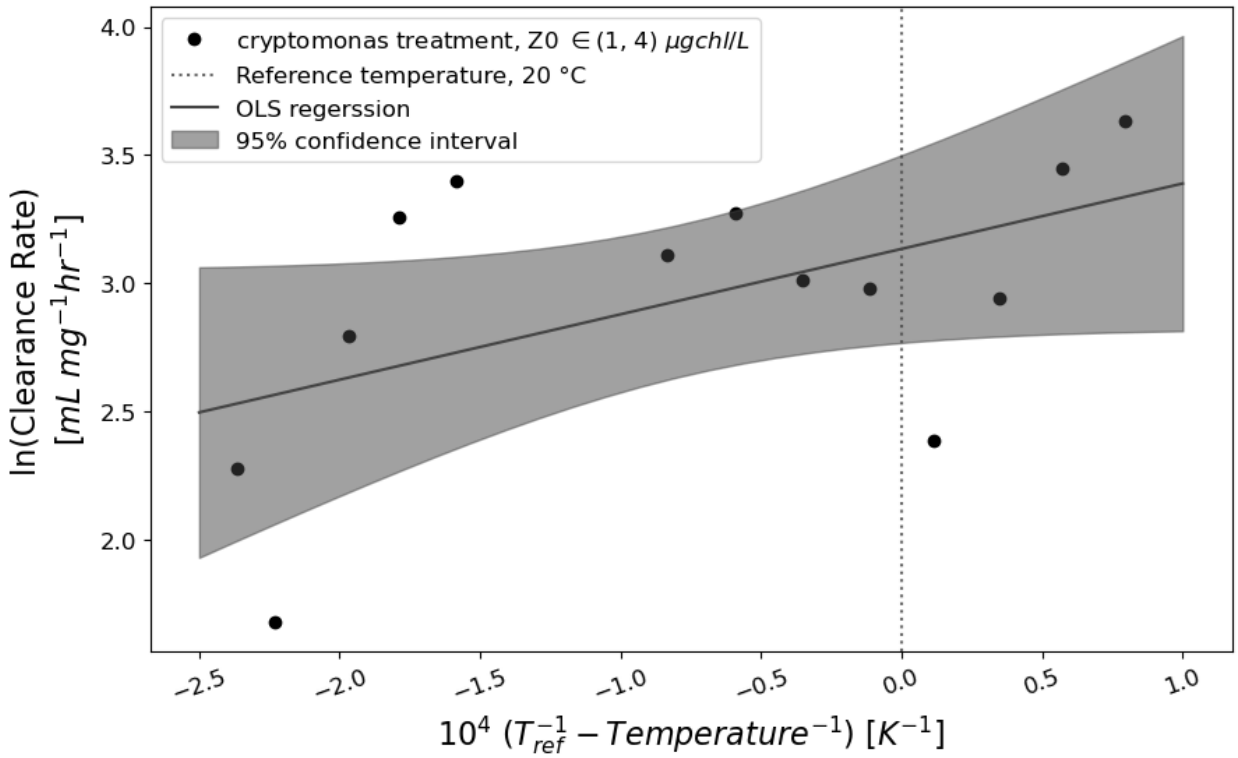

Figure 6. Experimental Quagga Mussel (*Dreissena rostriformis bugensis)* clearance rates (natural log-transformed) by inverse reference temperature minus inverse temperature (*K*). Data source: Vanderploeg et al. (2010).

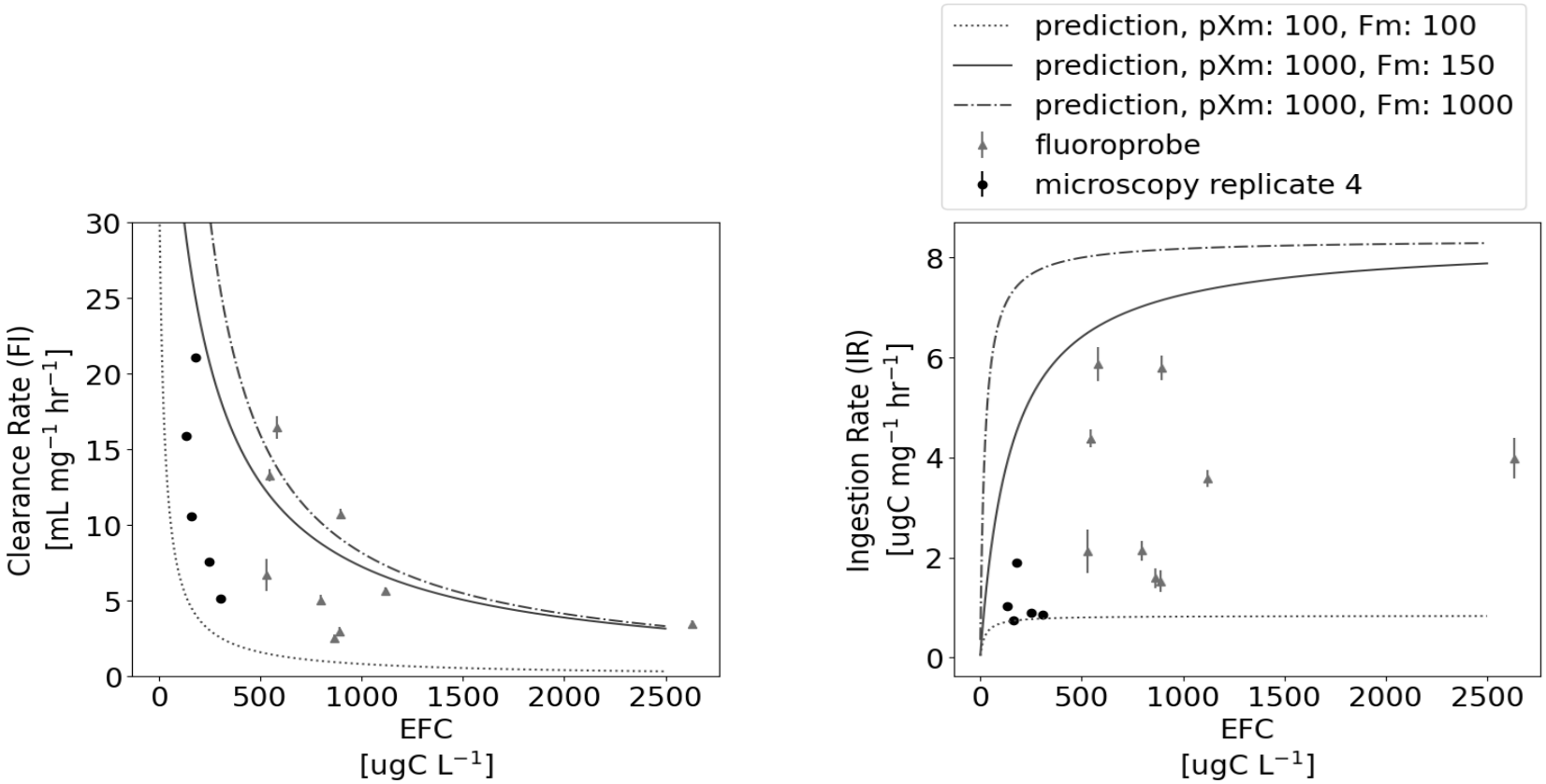

Figure 7. Quagga Mussel (left) clearance rate (FI) and (right) ingestion rate (IR) model predictions (red lines) compared to experimental data (black dots represent microscopy measurements (Carrick et al., 2023), grey triangles represent FluoroProbe measurements (Vanderploeg et al., 2023), and whiskers represent standard error). Corrections to experimental data include a temperature correction (to 20°C) and a conversion of the observed IR using effective food concentration from Table 4. The Vanderploeg et al. (2010) experimentally informed parameter prediction is represented by a solid line, the low model prediction is represented by a dotted line, and the high model prediction is represented by a dash-dotted line. pXm represents surface area-specific ingestion rate ($\{\dot{p}_{Xm}\}$; J d^{-1} cm^{-2}) and Fm represents surface area-specific searching rate ($\{\dot{F}_m\}$; L d^{-1} cm^{-2}). The model simulation assumes an organism of 1.9 cm and a corresponding ash free dry weight of 20.82 mg.

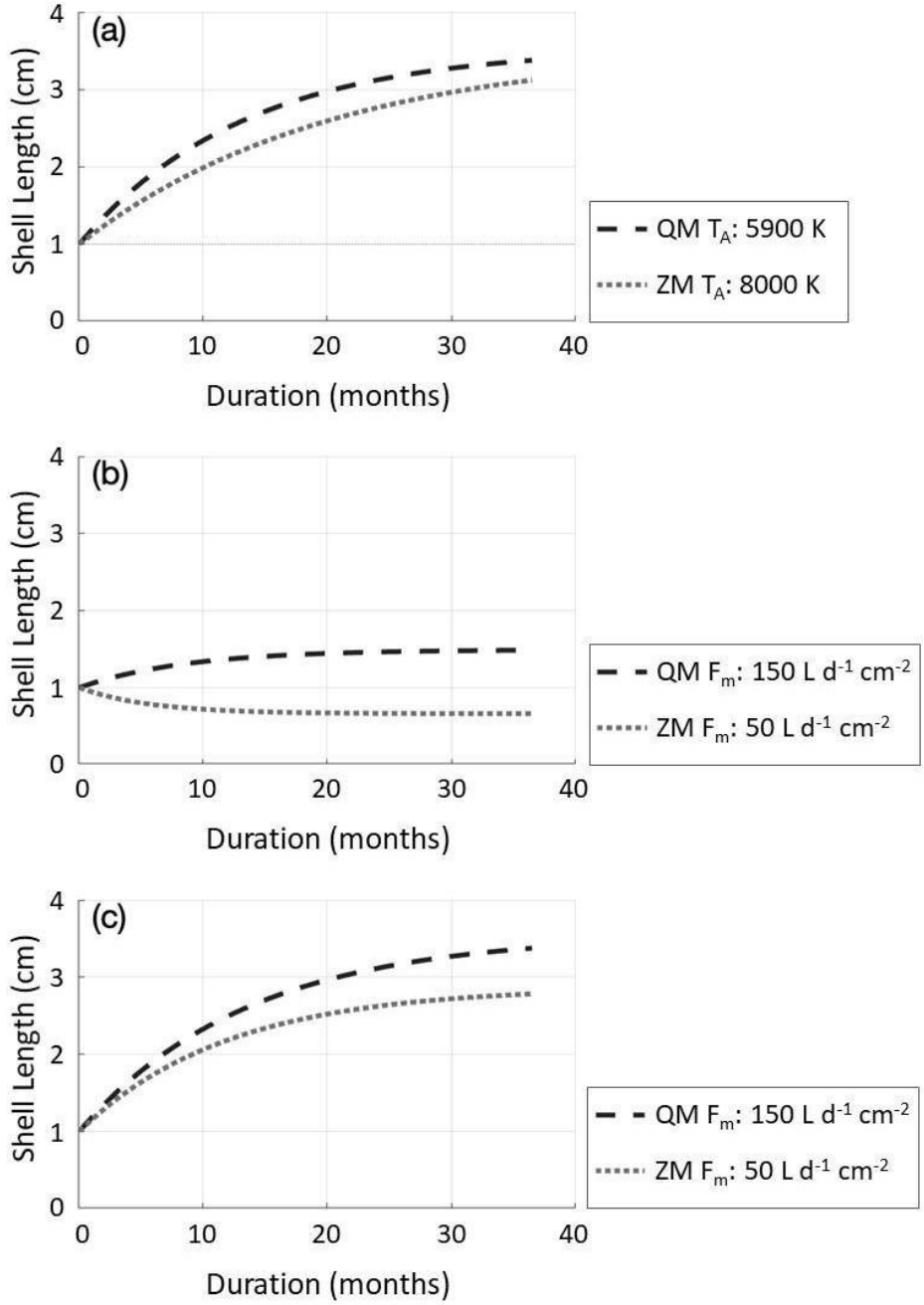

Figure 8. Model simulations of mussel growth using different dynamic energy budget parameter estimations for (a) Arrhenius temperature (T_A) with abundant food conditions, (b) maximum searching rate ($\{\dot{F}_m\}$) with low food conditions, and (c) $\{\dot{F}_m\}$ with abundant food conditions. Parameter estimates were chosen to illustrate the difference between Quagga (QM; *Dreissena rostriformis bugensis*) and Zebra Mussels (ZM; *D. polymorpha*). Environmental temperature for all simulations was 3.76°C. The low food concentration was 3.95 J L^{-1} (f = 0.37) and the abundant food concentration was 50.00 J L^{-1} (f = 0.88).

Supplementary Materials

Supplemental Table 1. Dynamic energy budget (DEB) parameters used for model simulations (if not otherwise specified in the manuscript). δ_M, T_A, $\{\dot{F}_m\}$, κ_X, and $[\dot{p}_M]$ were estimated in the current study. Other unestimated parameters are inferred from the AmP Zebra Mussel (AmP Collection, 2024), or from known common values.

Symbol	Description	Value	Units	Reference
δ_M	Shape coefficient	0.225	-	This study (Section 3.2.1)
T_A	Arrhenius temperature	6000	K	This study (Section 3.2.3)
T_H	Upper thermal limit	303.15	K	Garton et al. (2014)
T_{AH}	Arrhenius temperature for the rate of decrease at upper boundaries	80,000	K	T_A * 10
z	Zoom factor	0.58*	-	AmP Collection (2024)- Zebra Mussel corrected for difference in shape coefficients
$\{\dot{F}_m\}$	Maximum specific searching rate	150	L day^{-1} cm^{-2}	This study (Section 3.2.4)
κ_X	Digestion efficiency of food to reserve	0.09	-	This study
$\dot{v}$	Energy conductance	0.02	cm day^{-1}	AmP common value
κ	Allocation fraction to soma	0.99269	-	AmP Collection (2024)- Zebra Mussel
κ_R	Reproduction efficiency	0.95	-	AmP Collection (2024)- Zebra Mussel
$[\dot{p}_M]$	Volumetric-specific maintenance	154.2**	J day^{-1} cm^{-3}	This study
$\{\dot{p}_T\}$	Surface area-specific maintenance	0	J day^{-1} cm^{-2}	Exothermic animal
$\dot{k}_j$	Maturity maintenance rate coefficient	0.002	1 day^{-1}	AmP Collection (2024)- Zebra Mussel
E_G	Specific cost for structure	2349.0525	J cm^{-3}	AmP Collection (2024)- Zebra Mussel

E_H^b	Maturity at birth	2.203e-6	J	AmP Collection (2024)- Zebra Mussel
E_H^j	Maturity at metamorphosis	8.376e-6	J	AmP Collection (2024)- Zebra Mussel
E_H^p	Maturity at puberty	5.868e-1	J	AmP Collection (2024)- Zebra Mussel
$\dot{h}_a$	Weibull aging acceleration	1.937e-9	1 day^{-2}	AmP Collection (2024)- Zebra Mussel
S_G	Gompertz stress coefficient	0.0001	-	AmP Collection (2024)- Zebra Mussel

*z = 0.58, calculated from Zebra Mussel z (0.8787) multiplied by Zebra Mussel shape coefficient (0.34) and divided by Quagga Mussel shape coefficient (0.225, estimated in this study).

**$[\dot{p}_M]$ = 129.96, calculated based on the values of z, $\dot{v}$, κ, and $[E_m]$: $[\dot{p}_M] = \kappa * \{\dot{p}_{Am}\} / z = \kappa * [E_m] * \dot{v} / z$ (κ_p only needed for calculating nutrient flux).

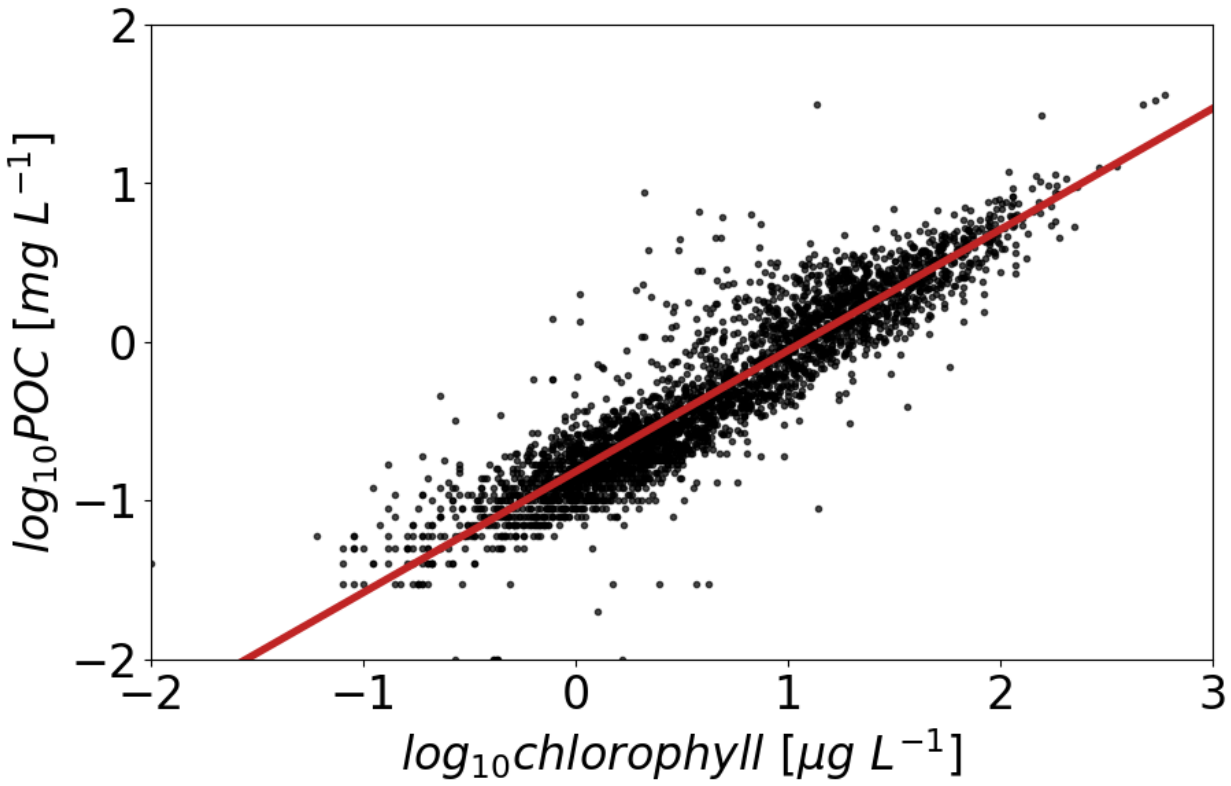

Supplemental Figure 1. Linear regressions between chlorophyll and particulate organic carbon (POC) concentrations. Black points are measurements from Lake Huron's Saginaw Bay, Lake Erie, and Lake Michigan. Chlorophyll and POC data were collected by the National Atmospheric and Ocean Administration Great Lakes Environmental Research Laboratory as part of a harmful algal bloom monitoring program (NOAA GLERL, 2024) and a long-term research program in Lake Michigan (Pothoven unpub. data). The red line is the ordinary least squares regression. The regression equation is: $log_{10}POC\ [mg\ L^{-1}] = (0.76 \pm 0.005) \times log_{10}chl\ [ug\ L^{-1}] - 0.82 \pm 0.005$ (regression $r^2 = 0.85$, numbers of observations = 3444, degrees of freedom = 1).

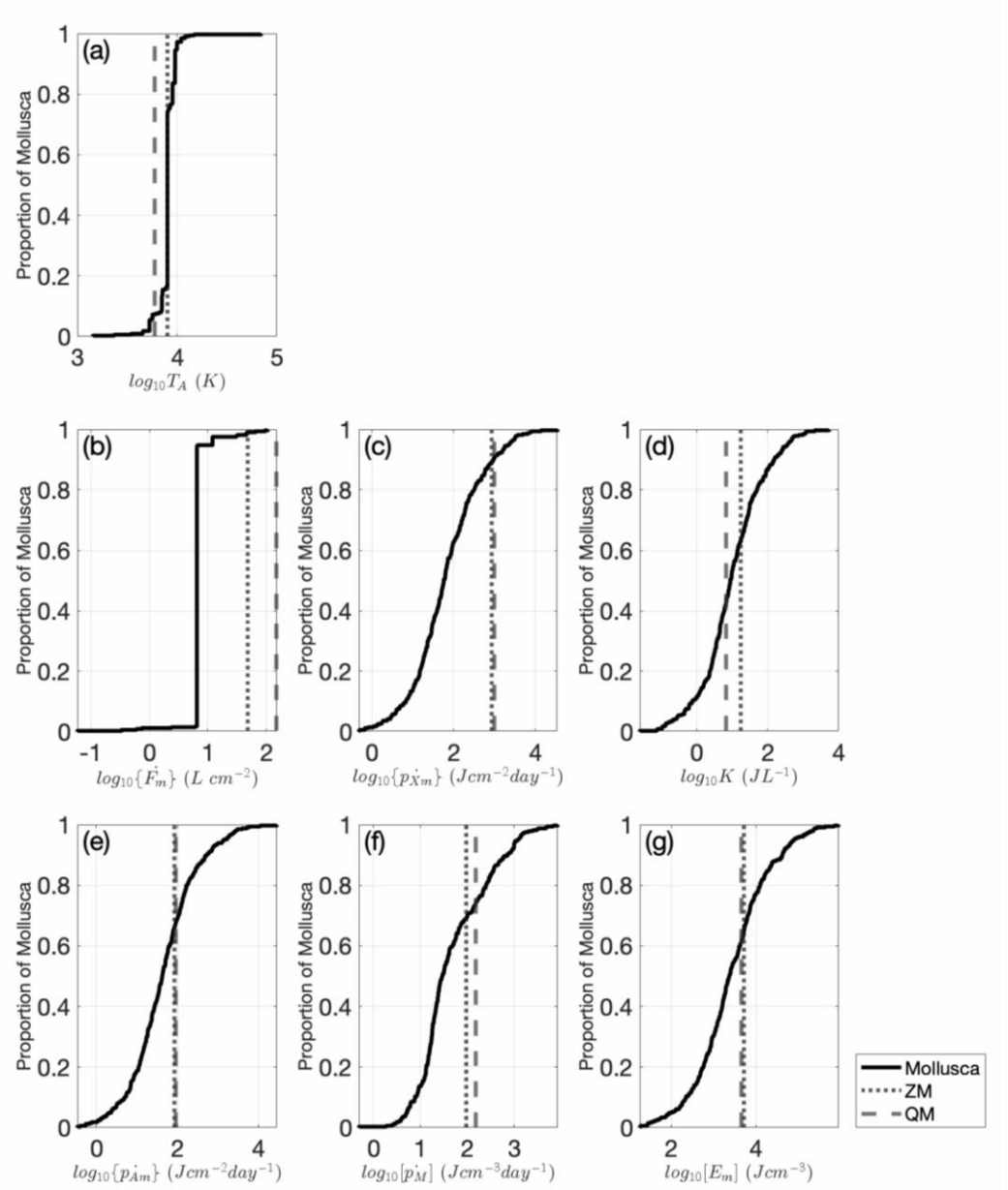

Supplemental Figure 2. Empirical Cumulative Distribution Function plots comparing the parameter estimates of eight dynamic energy budget parameters estimated in the current study to mollusk species obtained from the AmP Collection (2024). Parameters shown are (a) Arrhenius temperature (T_A), (b) maximum surface area-specific searching rate ($\{\dot{F}_m\}$), (c) maximum surface area-specific ingestion rate ($\{\dot{p}_{Xm}\}$), (d) half saturation coefficient (K), (e) maximum surface area-specific assimilation rate ($\{\dot{p}_{Am}\}$), (f) volume-specific maintenance ($[\dot{p}_M]$), and (g) energy density ($[E_M]$). Black lines denote the spread of parameter estimates for mollusks in the AmP collection. Vertical lines indicate the log of the parameter estimate in our study for Quagga Mussels (dashed; QM; *Dreissena rostriformis bugensis*) and parameter estimate from AmP for Zebra Mussels (dotted; ZM; *D. polymorpha*).